Molecular Therapy
Methods & Clinical Development
Original Article

Oxidative stress induced by sustained supraphysiological intrastriatal GDNF delivery is prevented by dose regulation

Marcelo Duarte Azevedo,[1] Naika Prince,[1,4] Marie Humbert-Claude,[1,5] Virginia Mesa-Infante,[2] Cheryl Jeanneret,[1] Valentine Golzne,[1] Kevin De Matos,[1,6,7,8] Benjamin Boury Jamot,[3] Fulvio Magara,[3] Tomas Gonzalez-Hernandez,[2] and Liliane Tenenbaum[1]

[1]Laboratory of Cellular and Molecular Neurotherapies, Center for Neuroscience Research, Clinical Neurosciences Department, Lausanne University Hospital (CHUV) and University of Lausanne (UNIL), 1011 Lausanne, Switzerland; [2]Departamento de Ciencias Médicas Básicas, Facultad de Ciencias de la Salud, Instituto de Tecnologías Biomédicas (ITB), Universidad de La Laguna, La Laguna, 38200 Tenerife, Spain; [3]Center for the Study of Behaviour, Department of Psychiatry, Lausanne University Hospital and University of Lausanne (CHUV-UNIL), 1008 Lausanne, Switzerland

Despite its established neuroprotective effect on dopaminergic neurons and encouraging phase I results, intraputaminal GDNF administration failed to demonstrate significant clinical benefits in Parkinson's disease patients. Different human GDNF doses were delivered in the striatum of rats with a progressive 6-hydroxydopamine lesion using a sensitive doxycycline-regulated AAV vector. GDNF treatment was applied either continuously or intermittently (2 weeks on/2 weeks off) during 17 weeks. Stable reduction of motor impairments as well as increased number of dopaminergic neurons and striatal innervation were obtained with a GDNF dose equivalent to 3- and 10-fold the rat endogenous level. In contrast, a 20-fold increased GDNF level only temporarily provided motor benefits and neurons were not spared. Strikingly, oxidized DNA in the substantia nigra increased by 50% with 20-fold, but not 3-fold GDNF treatment. In addition, only low-dose GDNF allowed to preserve dopaminergic neuron cell size. Finally, aberrant dopaminergic fiber sprouting was observed with 20-fold GDNF but not at lower doses. Intermittent 20-fold GDNF treatment allowed to avoid toxicity and spare dopaminergic neurons but did not restore their cell size. Our data suggest that maintaining GDNF concentration under a threshold generating oxidative stress is a pre-requisite to obtain significant symptomatic relief and neuroprotection.

INTRODUCTION

The main hallmark of Parkinson's disease (PD) is the preferential loss of nigrostriatal dopaminergic (DA) neurons. Glial cell line-derived neurotrophic factor (GDNF) was shown to enhance neuronal survival through RET signaling when applied before[1,2] or after[3,4] an insult to DA neurons.

However, exogenously applied GDNF also acts as a booster of the DA pathway. It enhances K^+-induced dopamine release,[5,6] a phenomenon that has been related to an increase in number of DA neuron synapses[7] or synaptic activity by potentiation of calcium channels.[8] Furthermore, GDNF treatment increases the activity of tyrosine hydroxylase (TH), the main enzyme of dopamine biosynthesis.[9] Accordingly, high-dose GDNF delivery in the putamen of marmosets has been shown to drastically increase the tissue level of dopamine and its metabolites.[10]

After long-term uninterrupted treatment, compensatory effects appear, altering dopamine homeostasis through neurochemical effects such as TH transcription downregulation.[9,11,12] Interestingly, it has been shown that pulsed GDNF treatment does not cause TH downregulation.[13]

A small (2- to 3-fold) lifelong GDNF overexpression from its endogenous locus in transgenic mice increased DAT activity.[14] In contrast, when applied in adult rats using an AAV vector, GDNF reduced DAT activity.[15] This apparent discrepancy might result from different life

Received 25 January 2023; accepted 6 September 2023;
https://doi.org/10.1016/j.omtm.2023.09.002.

[4]Present address: Division of Pharmacology, Utrecht Institute for Pharmaceutical Sciences, Faculty of Science, Utrecht University, 3584 CG Utrecht, the Netherlands

[5]Present address: Pharmacie des Hôpitaux de l'Est Lémanique, 1847 Rennaz, Switzerland

[6]Present address: Sorbonne Université, Institut du Cerveau - Paris Brain Institute - ICM, CNRS, Inria, Inserm, AP-HP, Hôpital de la Pitié Salpêtrière, 75013 Paris, France

[7]Present address: CIBM Center for Biomedical Imaging, Lausanne, Switzerland

[8]Present address: Radiology Department, Lausanne University and University Hospital, Lausanne, Switzerland

Correspondence: Marcelo Duarte Azevedo, Laboratory of Cellular and Molecular Neurotherapies, Center for Neuroscience Research, Clinical Neurosciences Department, Lausanne University Hospital, 1011 Lausanne, Switzerland.
E-mail: marcelo-duarte-azevedo@hotmail.com
Correspondence: Liliane Tenenbaum, Laboratory of Cellular and Molecular Neurotherapies, Center for Neuroscience Research, Clinical Neurosciences Department, Lausanne University Hospital, 1011 Lausanne, Switzerland.
E-mail: liliane.tenenbaum@chuv.ch

periods for GDNF overexpression onset, different cell types expressing GDNF, or regulation of an endogenous GDNF promoter absent in viral vectors. A decrease of DAT activity results in a high synaptic dopamine level and increased dopamine catabolism generating an excess of free radicals.[16] Consequently, sustained high-dose GDNF that results in dopamine dyshomeostasis[10] could possibly compromise neuronal survival, thus reducing the beneficial outputs of RET signaling activation.

The confirmation that PD patients' remaining DA neurons still express RET and contain phosphorylated ribosomal S6 protein (a RET signaling output), although at a lower level, supports the feasibility of a GDNF-mediated neuroprotective approach.[17] However, reduced activation of the RET pro-survival signaling pathway in response to long-term GDNF treatment of DA neuron primary cultures has been reported,[18] suggesting that GDNF neuroprotective effects could decrease over time.

GDNF and its related factor neurturin, have been evaluated in clinical trials for PD.[19,20] Although the initial phase I clinical trials generated large expectations,[21,22] further placebo-controlled trials failed to demonstrate clinical benefits.[19,20,23] Nevertheless, positron-emission tomography (PET) scan imaging of AAV-GDNF-treated patients have demonstrated clear functional improvements[23,24] and postmortem samples of AAV-neurturin-treated patients have revealed regrowth of DA neuronal fibers at the site of delivery.[25–27] Since clinical trials consisted of long-term unregulated GDNF/NRTN administration, it could be that, despite the presence of a pro-survival RET signaling, symptomatic relief has been compromised by perturbed dopamine dyshomeostasis as demonstrated in pre-clinical models. Therefore, a better knowledge of GDNF mechanism of action *in vivo* in complex neuronal circuits is needed to revisit the clinical paradigm.

Using a doxycycline (dox)-inducible AAV vector, we have previously shown that a low striatal GDNF concentration (∼50 pg/mg tissue, i.e., ∼ 5-fold the endogenous level) was sufficient to induce RET signaling in healthy rats in the absence of undesirable effects. In contrast, higher GDNF concentration induced TH downregulation (from ∼200 pg/mg tissue) and contralateral amphetamine-induced rotations (from ∼1,000 pg/mg tissue).[28]

In this study, we aimed to determine whether a pharmacologically controlled GDNF treatment could increase motor benefits while avoiding undesired neurochemical effects. We demonstrate, in a partial 6-hydroxydopamine (6-OHDA) rat model, that continuous administration of high-dose GDNF (20-fold the endogenous level) failed to provide significant neuronal protection and sustained behavioral improvement and resulted a 50% increased level of oxidized DNA in the substantia nigra pars compacta (SNc) and aberrant sprouting.[29] In contrast, a low-dose (3-fold the endogenous level) or an intermittent high-dose treatment resulted in DA neuron protection and motor symptom reduction, without inducing deleterious effects.

RESULTS

Modulation of striatal GDNF transgene expression by oral dox treatment

High doses of 6-OHDA injected in a single site in the striatum result in lesions that regress over time,[4,30] whereas low doses delivered in multiple sites induce progressive lesions.[30,31] Ten micrograms of 6-OHDA distributed in four delivery sites was injected in the right striatum (Figure S1) 1 week before AAV2/5-V16-*hGDNF* (Figure 1A). With this experimental scheme, the lesion was partial (∼60% reduction of TH staining; Figures S1A and S1B) and behavioral asymmetry was slowly progressive (Figures S1C and 2B). As expected, the reduction of striatal TH staining relative to the intact side correlated with the number of turns (Figure S1D). GDNF expression started 1 week post-vector injection, i.e., 2 weeks post-toxin injection, thus during the progressive phase of the lesion (Figure S2).

Using the AAV-V16 vector, GDNF intrastriatal dose can be modulated over 2 orders of magnitude, depending on the dox dose and the amount of vector injected.[28] Two experimental groups were evaluated: a "high-dose" group injected with $1.0–1.8 \times 10^{10}$ GDNF transducing units (T.U.) and treated with dox diet at a concentration of 500 mg/kg and a "low-dose" group injected with 4.1×10^{9} GDNF T.U. and treated with dox diet at a concentration of 200 mg/kg (Figure 1B). In the high-dose group, different dox treatment regimens were applied during 16 weeks after AAV2/5-V16-*hGDNF* injection: no treatment and continuous (Cont.) or intermittent (Int.) treatment. In the low-dose group, animals were given continuously 200 mg dox/kg diet or left untreated. The control group received a continuous dox treatment (Figures 1A and 1B).

GDNF levels in the striatum were measured using ELISA assays. In the AAV2/5-V16-*hGDNF* dox-untreated groups, 28.4 and 25.4 pg/mg hGDNF were measured, respectively, in the high- and low-dose groups (i.e., ∼3-fold the rat GDNF endogenous level). In the groups treated with dox at 200 and 500 mg/kg dox, hGDNF concentrations were 103.7 and 186.8 pg/mg tissue (∼10- and ∼20-fold of the rat GDNF level, respectively). In the intermittently treated group, dox treatment was interrupted 1 week before euthanasia, allowing reversal to the level of the untreated group (Figure S2). For simplicity, hereafter the rat groups are referred to as GDNF 20×, GDNF 20× Int., GDNF 10×, GDNF 3×, and GFP.

The distribution of the GDNF transgene product demonstrated by immunohistochemistry covered most of the striatum (Figure 1C).

Initial motor symptom relief mediated by high-dose GDNF intrastriatal administration is lost after long-term treatment

Motor asymmetry was evaluated using the amphetamine-induced rotation test. The number of ipsilateral turns was significantly increased between 3 and 16 weeks in the GFP group indicating that neurodegeneration is progressive in this form of 6-OHDA lesion (Figure 2B). A comparison between the different experimental groups revealed a partial and non-significant reduction of the turns in the

A

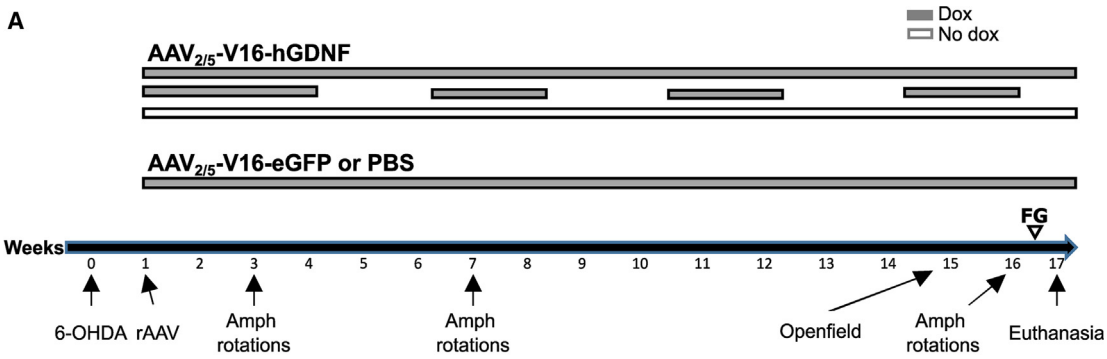

B

Experimental groups	AAV dose (T.U.)	Dox dose (mg/kg diet)	hGDNF (pg/mg tissue) (-fold endogenous)	FG	Behavioural test
High dose	1.0×10^{10}	0	28.41 ± 22.77 (3X)	X	Amphetamine-induced rotations
		500 Cont.	186.83 ± 65.05 (20X)		
		500 Int.	30.10 ± 9.90 (20X Int.)		
	Control[§]	500 Cont.	9.46 ± 1.26 (rGDNF)		
Low dose	4.1×10^{9}	0	25.46 ± 13.46 (3X)	NT	Amphetamine-induced rotations Openfield
		200 Cont.	103.71 ± 67.24 (10X)		
	PBS	200 Cont.	NT		

C

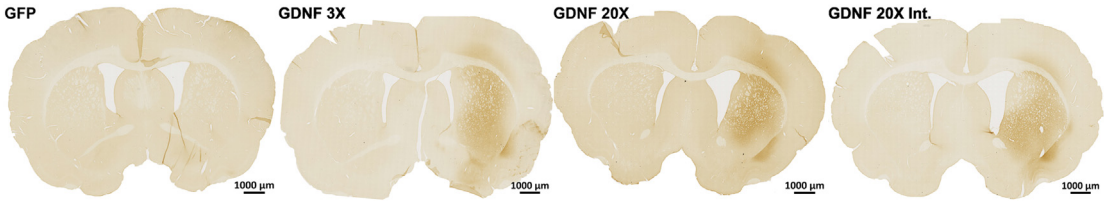

Figure 1. Experimental design.

(A) Experimental scheme. Two independent experiments (high dose and low dose) using different vector amounts and dox concentrations were performed. All rats were injected with 10 µg of 6-OHDA in four delivery sites (see Figure S1). One week later, AAV vectors or PBS were injected at the same coordinates. Amphetamine-induced rotational behavior was evaluated at 3, 7, and 16 weeks post-6-OHDA injection. Drug-free open-field motor behavior was also assessed in the low-dose experiment at 15 weeks post-6-OHDA injection. Some of the animals from the high-dose group received intrastriatal FluoroGold (FG) injections in the 16th week. Rats were euthanized at 17 weeks post-6-OHDA. Some of the animals were processed for protein extracts and the others for immunohistology. (B) Detailed description of the experiments and striatal GDNF concentrations. AAV2/5-V16-*hGDNF* batches were matched based on a functional assay (Table S1). [§]AAV2/5-V16-*eGFP* was titer-matched with AAV2/5-V16-*hGDNF* based on the number of viral genomes (vg); the value indicated represents endogenous rat GDNF. The dox treatment was administered in the food pellets and the dox dose used for each experimental group is indicated in the third column. GDNF striatal concentrations are vector-expressed hGDNF obtained after subtracting the rat GDNF endogenous level. Means and SD are shown. For simplicity, the groups were designated by the amount of vector-expressed hGDNF relative to endogenous rat GDNF amount. The retrograde tracer FG was used in part of each experimental group of the high-dose experiment but not in the low-dose experiment. Amphetamine-induced rotations were evaluated in both experiments, whereas open-field motor behavior was only assessed in the low-dose experiment. (C) GDNF localization in the striatum. Striatal sections were labeled with an antibody recognizing human GDNF. Representative sections for the GFP, GDNF 3×, GDNF 20×, and GDNF 20× Int. groups are shown. Scale bars, 1,000 µm. Data were generated in the high-dose experiment. NT, not tested.

GDNF 3× and GDNF 20× Int. groups at 3 weeks post-6-OHDA injection (Figure 2A). This difference became significant with complete correction of behavioral asymmetry at 7 weeks in the 20× Int. group, and in both the 3× and GDNF 20× Int. groups at 16 weeks post-lesion (Figure 2A). Unlike these two experimental groups, rats of the GDNF 20× group showed complete recovery of symmetry at

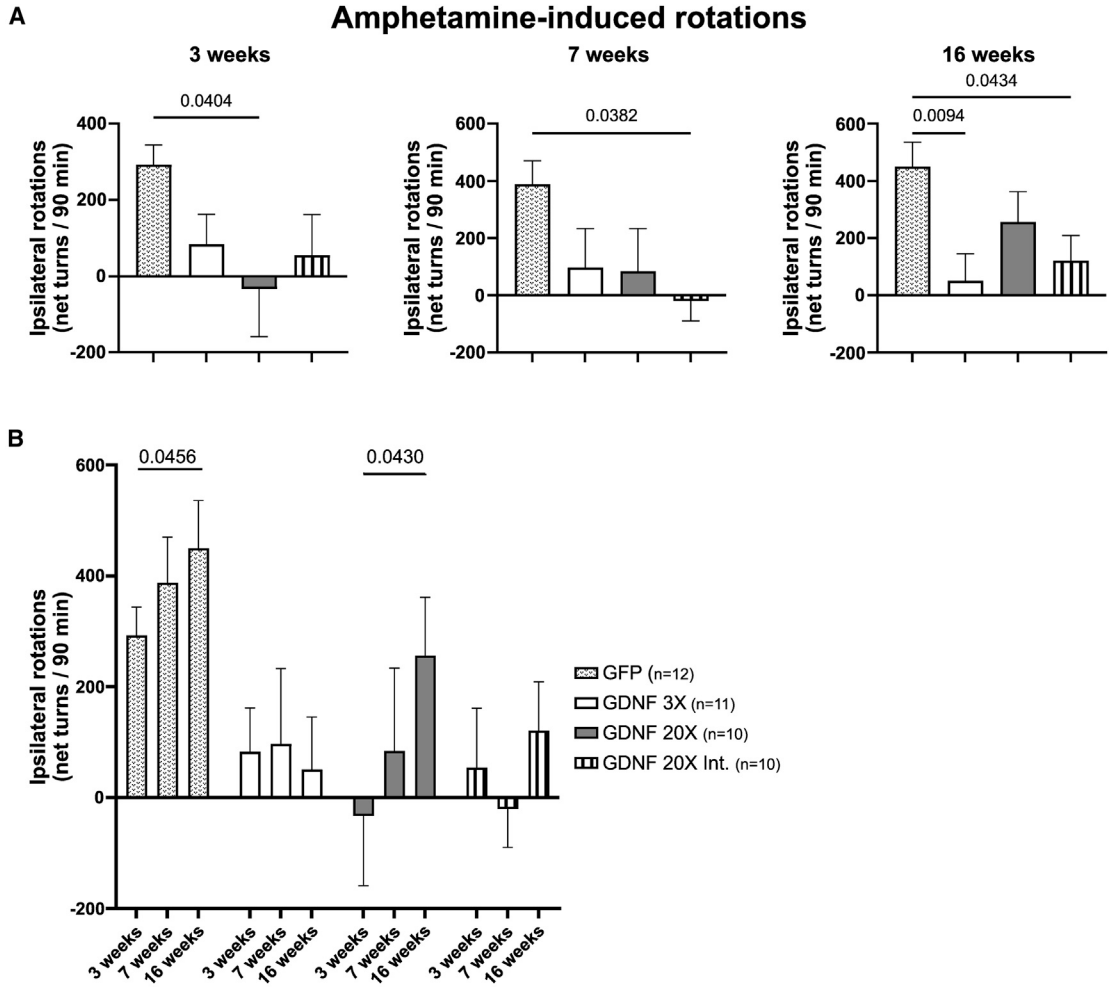

Figure 2. Long-term persistence of motor symptoms relief depends on the GDNF treatment regimen

(A) Correction of asymmetric amphetamine-induced rotational behavior. The animals were injected intraperitoneally with amphetamine (2.5 mg/kg), harnessed to the rotameter. The number of turns was measured using the Fusion software for 90 min at 3, 7, and 16 weeks post-6-OHDA injection. Statistical analysis was performed using one-way ANOVA followed by Dunnett's multiple comparisons test (all groups were compared with the GFP group). Means and SD are shown. (B) Kinetics of behavioral effects. Statistical analysis was performed using two-way ANOVA followed by Dunnett's multiple comparisons test (the different time points were compared within each group). Means and SD are shown.

3 weeks post-6-OHDA injection (Figure 2A). However, thereafter they underwent a progressive return to asymmetry, with a rotation number not significantly lower than the GFP group (Figure 2A). This suggests that, in contrast with GDNF 3× and GDNF 20× Int., sustained GDNF 20-fold treatment did not halt the progression of motor symptoms. Confirming this interpretation, for the GDNF 20× group, the number of turns significantly increased between 3 and 16 weeks, whereas for the GDNF 3× and GDNF 20× Int. groups, the asymmetry did not increase during the same period (Figure 2B).

Dose- and schedule-dependent GDNF-mediated protection of the nigrostriatal DA pathway

The lack of behavioral recovery after continuous treatment with a high GDNF dose could be explained by a lower survival of DA neurons, less preserved DA innervation, and/or neurochemical effects affecting DA neurotransmission.

DA neurons were examined using immunofluorescence. TH is not a suitable marker to evaluate DA neuron survival since its transcription is downregulated by GDNF.[11,12,29] In accordance to previously published data, the number of nigral TH+ cells (Figure 3A) as well as striatal TH protein amount (Figure 3B) were significantly reduced in the GDNF 20× group. However, a lower (3×) GDNF dose or intermittent treatment did not significantly affect either TH+ cells numbers or striatal TH. Therefore, vesicular monoamine transporter-2 (VMAT2) marker was considered. To determine whether VMAT2 labeling reliably reflects surviving nigral DA neurons in our settings, the retrograde tracer FluoroGold (FG) was

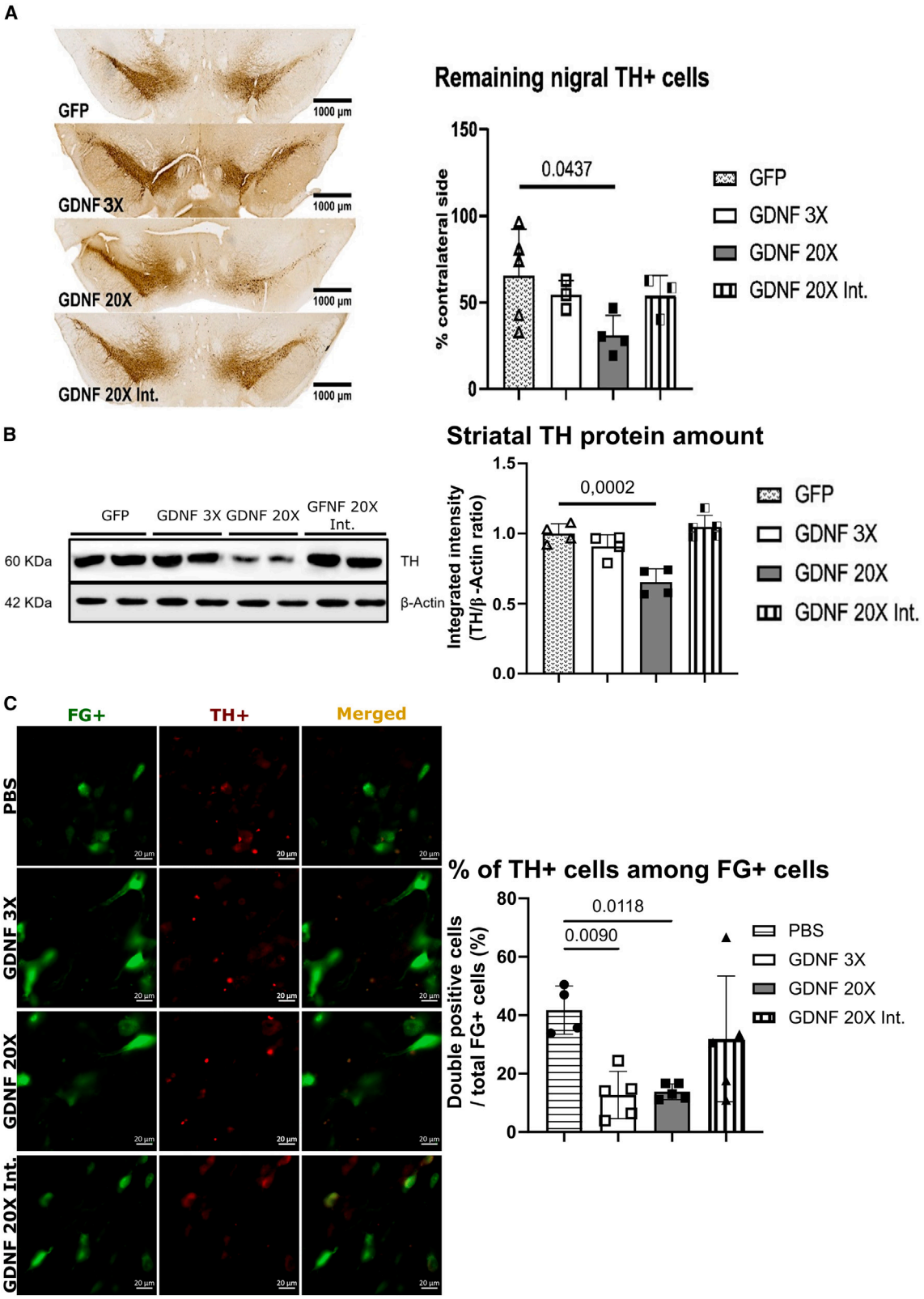

(legend on next page)

injected into the striatum (Figure 1B; high-dose experiment). FG+ cells in the SNc are DA neurons that have maintained the capacity for retrograde transport from the striatum to the SNc. The proportion of FG+ cells that were TH+ was significantly reduced (~3-fold) in both the GDNF 3× and GDNF 20× groups (Figure 3C), suggesting that a large proportion of retrogradely labeled DA neurons did not express TH at a detectable level after GDNF treatment. In contrast, the proportion of FG/VMAT2 double-labeled cells was similar in all groups (Figure 4A), confirming that VMAT2 marker is not affected by GDNF.

The number of VMAT2+ cells in the SNc of the lesioned side relative to the contralateral side was significantly increased (~2-fold) in the GDNF 20× Int. group in comparison with the GFP group, whereas there was no significant difference for the GDNF 20× and GDNF 3× groups (Figure 4B). It should be noted that, in the GDNF 3× group, the percentage of remaining cells was ~1.4-fold increased. The lack of significance ($p = 0.2646$) in this group could be due to the small sample size ($n = 3$). Indeed, in the low-dose experiment, GDNF 3× treatment resulted in a significantly increased VMAT2+ cell number (~2-fold; $p = 0.0458$; $n = 5$) (Figure 6C). As expected, TH staining failed to reveal an increased number of surviving neurons in the GDNF 20× Int. and GDNF 3× groups as demonstrated with VMAT-2 staining (Figure 3A).

It has been shown that DA neurons with larger soma and wider terminal arborization are more susceptible to degeneration in PD[32–34] and more vulnerable to DA toxin insults in pre-clinical models.[35,36] Indeed, Healy-Stoffel et al.[36] have observed a 13% decrease of the mean DA neuron cell size in the SNc following intrastriatal 6-OHDA injection. Furthermore, a study in monkeys indicates that GDNF infusion may protect large-sized DA neurons from MPTP toxicity.[37] To confirm these observations under our conditions, the DA neuron surface was compared in the right and left SNc of the control (GFP) group. A reduced mean VMAT2+ cell size tendency was observed (Figure S1E). The analysis of cell size in our study revealed that the area of VMAT2+ cells in the lesioned side SNc was significantly higher in GDNF 3× rats than in GFP rats (Figure 4C). In contrast, no significant increase was observed in GDNF 20× and GDNF 20× Int. animals.

Next, we evaluated the remaining striatal DA innervation. Striatal VMAT2 staining was significantly increased in GDNF 20× Int. but not in GDNF 20× rats (Figure S3A). For the GDNF 3× group, although the mean and SD (85.67% ± 8.15%) were similar to the GDNF 20× Int. group (86.80% ± 8.96%), the increase was not significant ($p = 0.0982$), possibly due to the small number of samples tested ($n = 3$). Nevertheless, a significant inverse correlation was found between the number of amphetamine-induced ipsilateral turns and the VMAT2 remaining stained, suggesting that motor improvements were related to fiber preservation.

Since quantification of immunohistochemical staining intensity is subjected to saturating effects, striatal VMAT2 levels were further investigated by western blotting. Compared with the GFP group, VMAT2 levels were significantly increased in both the GDNF 3× and GDNF 20× Int. groups. Strikingly, in the GDNF 20× group, striatal VMAT2 levels were significantly decreased, suggesting that, at this dose, long-term GDNF treatment was deleterious for DA fibers (Figure 4D).

Supraphysiological GDNF treatment generates oxidative stress and aberrant sprouting

Long-term GDNF treatment increases striatal dopamine levels.[4] In view of dopamine's oxidative properties, we examined oxidative stress levels using 8-oxo-2′-deoxyguanosine (8-oxo-dG) immunostaining of nigral sections. The mean fluorescence intensity per cell was ~1.5-fold higher in the GDNF 20× group than that in the control group. No statistically significant differences versus the control group were observed among the other GDNF-treated groups (Figure 5A).

Our findings strongly suggest that a sustained supraphysiological GDNF treatment generates oxidative stress, resulting in the loss of neuroprotective effects on DA neurons.

GDNF-induced "aberrant sprouting," i.e., fiber sprouting in regions that are intrinsically devoid of or with light DA innervation, was appointed as a probable functionally detrimental effect counteracting the functional output of GDNF-induced striatal DA afference regeneration.[29] Therefore, we have evaluated DA sprouting in the substantia nigra pars reticulata (SNr) by comparing the VMAT2 immunostaining in the ipsilateral versus the contralateral side. A ~4-fold

Figure 3. TH downregulation in the presence of GDNF

(A) Midbrain sections were labeled with anti-TH antibodies followed by a secondary antibody coupled to biotin. The staining was revealed using streptavidin/peroxidase staining (left panel). The number of TH+ cells were counted on the ipsilateral and contralateral SNc at the same AP level, i.e., between −5.20 and −5.30. The number of TH-expressing cells in the ipsilateral SNc relative to the contralateral side is shown for the four groups of rats from the high-dose experiment. One-way ANOVA followed by Dunnett's multiple comparisons test (all groups were compared with the GFP group) revealed a statistically significant decrease of the percentage of remaining TH+ cells in the GDNF 20× group versus the control GFP group. In contrast, no statistically significant difference was observed between the GDNF 4× or GDNF 20× Int. and the GFP group. Means and SD are represented on the graphs (right panel). Scale bars, 1,000 μm. (B) Western blots of striatal proteins extracts from the high-dose experiment showing the amount of TH proteins. The 60 kDa bands were quantified using an ImageJ OD measurement tool. TH amounts relative to β-actin are shown. One-way ANOVA followed by Dunnett's multiple comparisons test (all groups were compared with the GFP group) ($n = 4$). (C) Some of the animals from the high-dose experiment were injected with FG retrograde tracer 1 week prior to euthanasia. Midbrain sections were labeled with anti-TH antibodies revealed with a secondary antibody coupled to Alexa Fluor 647. The total number of TH+ and FG+ cells were counted on the ipsilateral SNpc on five sections per animal. The proportion of TH+/FG+ double-labeled cells among the total number of FG+ cells was evaluated for each ipsilateral SNpc section. Means and SD are represented on the graphs. One-way ANOVA followed by Dunnett's multiple comparisons test (all groups were compared with the GFP group). Scale bars, 20 μm.

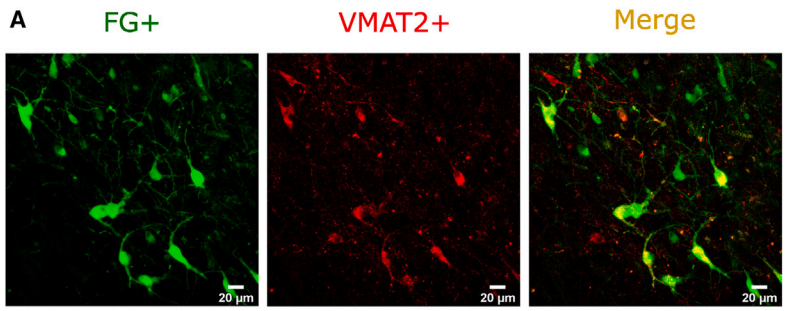

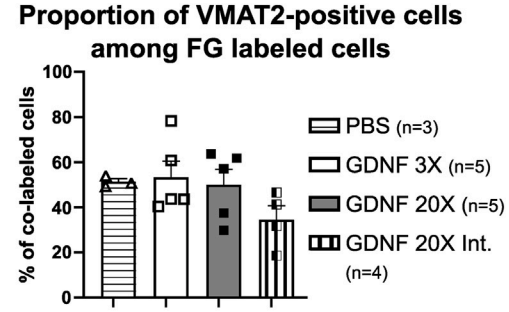

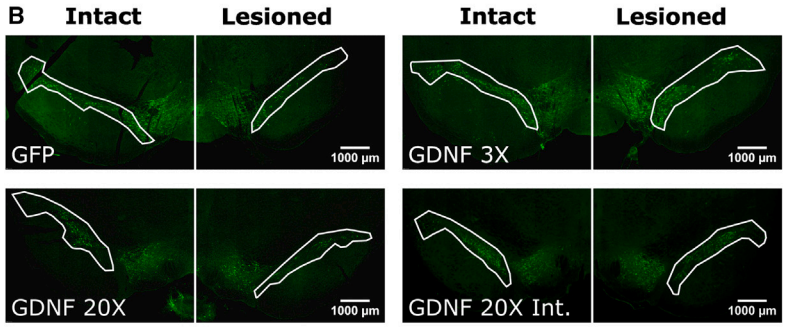

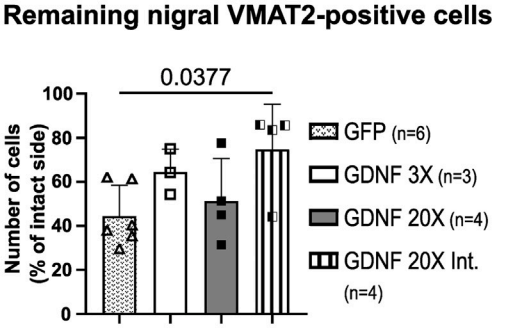

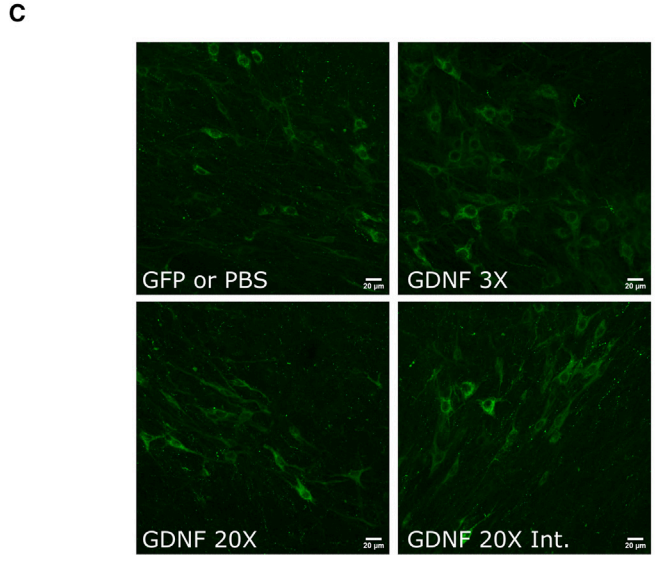

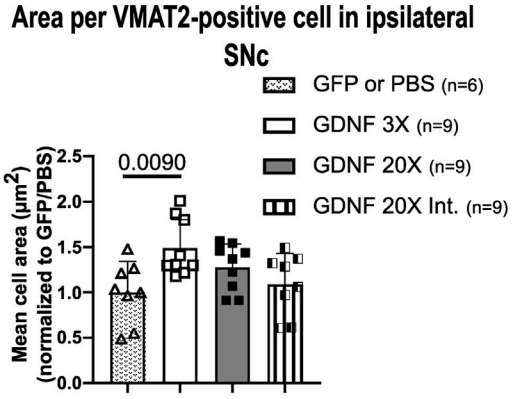

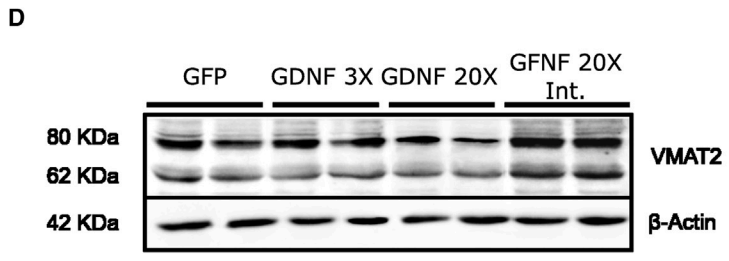

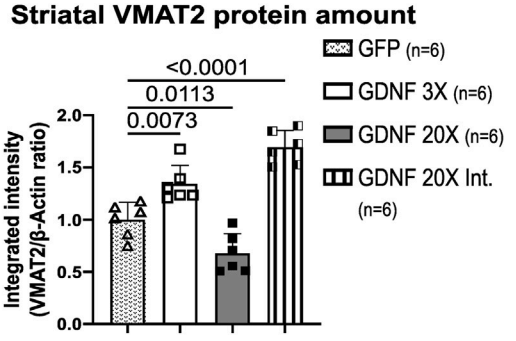

(legend on next page)

mean increase of the area covered by VMAT2 staining in SNr was observed in the GDNF 20× group (Figure 5B). It should be noted that out of four animals, two showed an increased VMAT2-stained area while the other two seemed similar to the control, suggesting that not all animals are affected by this deleterious effect. This inconsistent effect within the same group of animals could be due to different amount of dox ingested by the rats resulting in inter-individual variations of GDNF dose. A slight and non-significant increase was observed in the GDNF 20× Int. group. However, in one animal out of four, the increase was ∼3-fold, suggesting that aberrant sprouting was present in this animal and absent in the other three.

In summary, GDNF 3× allowed to preserve DA neuron number, size, and striatal innervation, as well as relieve motor symptoms, in the absence of oxidative stress and aberrant sprouting. In contrast, GDNF 20× did not protect neurons and terminals and elicited DNA damage and fiber sprouting in the SNr. GDNF 20× Int, provided motor benefits and preserved DA neuron number but not size, and aberrant sprouting was absent in the majority of the animals (Table 1).

Low-dose GDNF is sufficient to obtain symptomatic improvements in drug-free motor tests

In the low-dose experiment (Figure 1B), based on our previous study in healthy rats, the dox dose was set at 200 mg/kg diet, a clinically acceptable dose based on the comparison of plasmatic dox concentrations in patients and rats.[28] Following a recent publication,[38] we performed an additional calculation to evaluate the clinical applicability of the dox dose needed to induce GDNF beneficial effects in our study. A factor of 6.5 is used to translate rat doses into human doses. Therefore, a dose of 200 mg dox/kg diet (i.e., ∼4 mg/day per rat) corresponds to ∼25 mg/day for a human patient, which is lower than 40 mg/day, the dose administered for the treatment of rosacea and proven not to elicit adverse effects.[39,40]

The vector amount was adjusted to reach a concentration of ∼100 pg GDNF per mg tissue, previously shown to induce RET signaling without adverse effects.[28]

At 7 weeks post-lesion, an amphetamine-induced rotation test was performed. The motor symptoms in the GDNF 10× group were significantly reduced (∼2.5-fold) compared with the phosphate-buffered saline (PBS) group, whereas no significant effect was observed in the GDNF 3× animals (Figure 5A). At 16 weeks, the motor asymmetry was drastically (∼5-fold) and significantly reduced for both GDNF 10× and GDNF 3× animals.

To confirm these data in a drug-free motor test and in a restraint-free environment, the animals were placed in an open field and two different parameters were analyzed: total distance run and net ipsilateral rotations (Figure 6B). Both parameters were significantly improved in the GDNF 10× group, whereas for the GDNF 3× group only the total distance run was significantly increased.

These motor benefits were related to the preservation of VMAT2+ cells. Indeed, the number of remaining cells was significantly increased with both hGDNF doses (Figure 6C). Furthermore, striatal VMAT2+ staining inversely correlated with the number of amphetamine-induced turns (Figure S3B).

In conclusion, the AAV2/5-V16-hGDNF vector allowed to obtain motor benefits at 27 and 105 pg of vector-expressed hGDNF/mg tissue, 2 doses of hGDNF corresponding, respectively, to ∼3- and ∼10-fold of the endogenous rat GDNF concentration.

DISCUSSION

GDNF was discovered 30 years ago[41] and has been extensively studied, given the potent protection it confers to DA neurons[42] and motoneurons.[43]

Encouraging clinical improvements were first reported in two phase I clinical trials consisting of injecting GDNF recombinant protein into the putamen of PD patients: the Bristol study[21,44,45] and the Kentucky study[22,46] including, respectively, 5 and 10 patients. In these two initial trials, the UPDRS score (indicating the severity of the disease) decreased in all patients. Interestingly, PET scans showed increased fluoro-DOPA uptake[21] and TH+ fiber sprouting was observed post-mortem in one patient's putamen.[47] Disappointingly, in a further

Figure 4. Protection of nigrostriatal dopaminergic neurons depends on GDNF treatment regimen

(A) FG was injected in the striatum of 6-OHDA lesioned and AAV2/5-V16-*hGDNF* (or PBS)-treated rats 1 week before euthanasia (high-dose experiment). Midbrain sections were stained with anti-VMAT2 antibodies revealed by a secondary antibody coupled with cyanine 3 (red fluorescence). Green fluorescence, native FG fluorescence. The number of double-labeled cells and the total number of FG+ cells were counted on five sections (three random fields per section) per animal. The percentage of VMAT2-expressing cells among retrogradely labeled FG+ cells is shown for the four groups of rats from the high-dose experiment. Means and SD are given. One-way ANOVA followed by Dunnett's multiple comparisons test revealed no statistically significant difference between the groups (all groups were compared with the PBS group). Scale bars, 20 μm. (B) Midbrain sections were labeled with anti-VMAT2 antibodies revealed with a secondary antibody coupled to Alexa Fluor 488 (green fluorescence). The total number of VMAT2+ cells were counted on the ipsilateral and contralateral SNpc (the region is delineated in white) on five sections (three random fields per section) per animal. The percentage of VMAT2-expressing cells in the ipsilateral SNpc relative to the contralateral side is shown for the four groups of rats from the high-dose experiment. Means and SD are represented on the graphs. One-way ANOVA followed by Dunnett's multiple comparisons test (all groups were compared with the GFP group). Scale bars, 1,000 μm. (C) VMAT2+ cell area was measured using an ImageJ tool. Five midbrain sections and three fields per section were used for each animal. Means and SD are shown for each group of the high-dose experiment. One-way ANOVA followed by Dunnett's multiple comparisons test (all groups were compared with the mean of the GFP and PBS rats). Scale bars, 20 μm. (D) Western blots of striatal proteins extracts from the high-dose experiment showing the amount of VMAT2 proteins. VMAT2 isoforms (80 and 62 kDa) were quantified using an ImageJ OD measurement tool. Mean VMAT2 amounts relative to β-actin and SD are shown. One-way ANOVA followed by Dunnett's multiple comparisons test (all groups were compared with the GFP group).

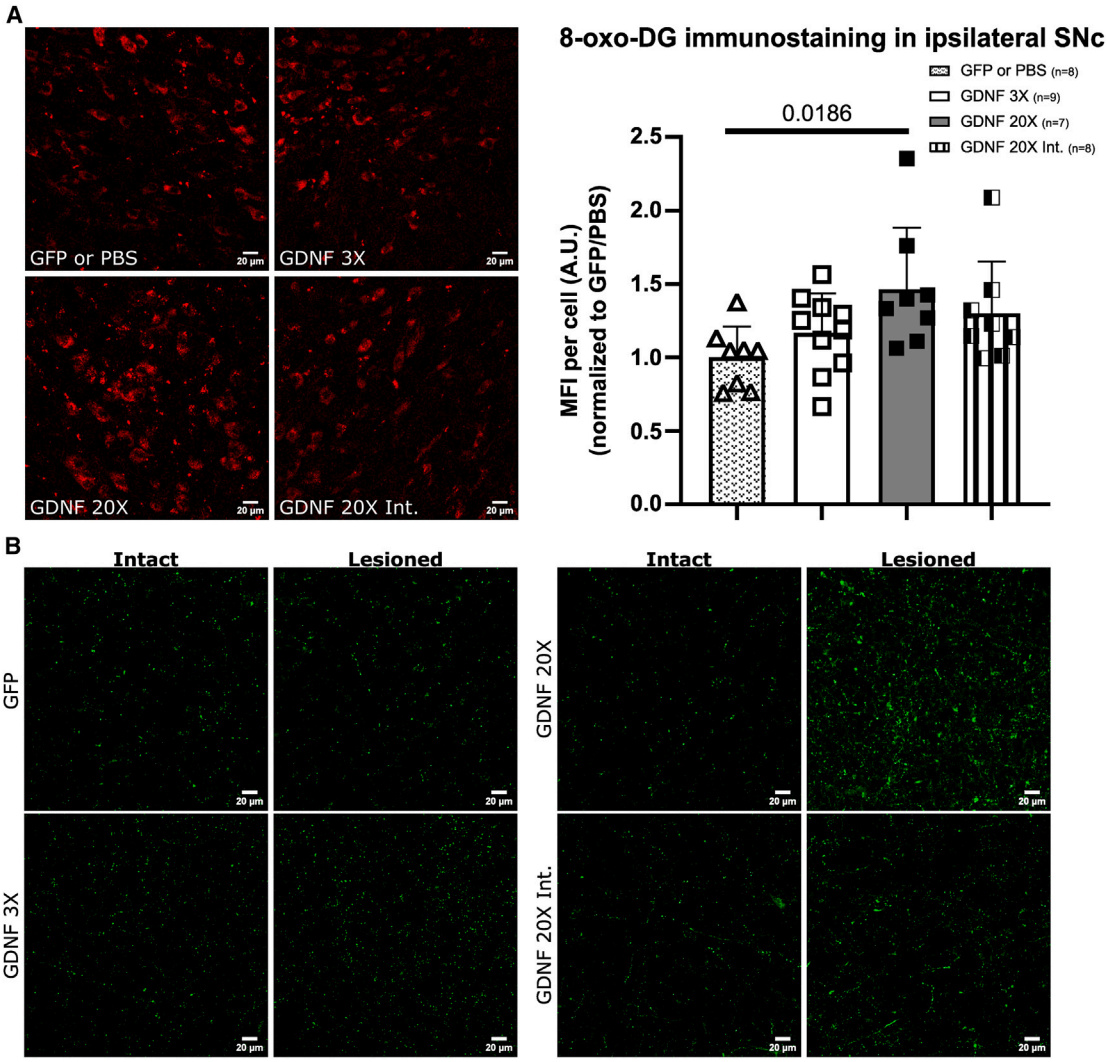

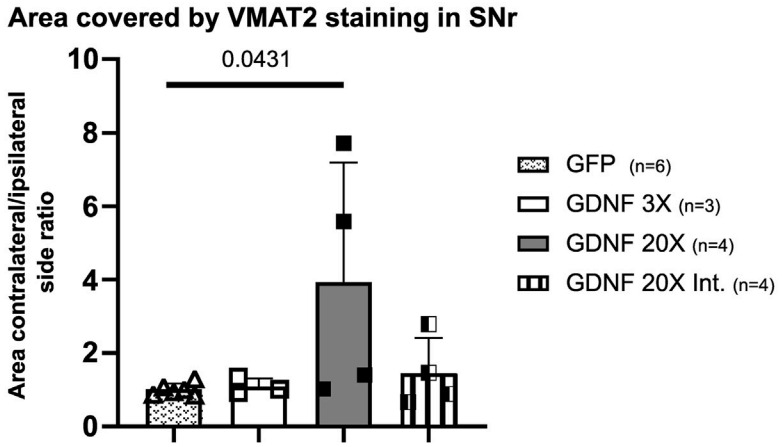

(legend on next page)

placebo-controlled trial GDNF failed to demonstrate clinical benefit.[20] In addition to a potential placebo effect, a limited coverage of the putamen could explain this failure to reproduce the encouraging phase I trial results.

Surprisingly, improved delivery methods, proven to allow a widespread putamen coverage failed to provide clinical benefits.[23,48] However, the dosage regimen used in the latter study drastically differed compared with the first trials. In the phase I Bristol study a dose escalation protocol with 14.4 and 28.8 mg daily for 2 successive periods of 6 months was performed. In the Kentucky study, an escalating dose of 3–10 to 30 mg/day for successive 8-week periods was applied. In contrast, in the latest phase II controlled study using MRI and convection-enhanced delivery,[23] patients received 10 intermittent treatments of 120 mg GDNF/putamen at 4-week intervals. Compared with the first trials, treatments were thus intermittent rather than continuous and the dose administered was 4- to 8-fold higher. Similar to the first placebo-controlled trial, no clinical benefit was demonstrated, although an increase in ^{18}F-fluoro-DOPA uptake in PET scans of treated patients, supporting functional improvement, was observed.[49] More recently, clinical trials using an AAV2 vector to deliver GDNF in the putamen resulted in similar observations, i.e., no significant clinical benefits despite a significant increase in ^{18}F-fluoro-DOPA uptake.[24]

Whether increased ^{18}F-fluoro-DOPA uptake in the putamen reflects increased DA neuron survival cannot be assumed in these studies. It may also reflect GDNF-mediated perturbations of DA re-uptake rather than increased fiber innervation. Indeed, numerous and sometimes contradictory neurochemical effects of sustained GDNF treatment have been described in animals, including decreased[15] or increased[14,50] DAT activity, TH transcriptional downregulation,[12,29] and inhibition of RET signaling.[18] Using the dox-inducible system described in this study, it has been demonstrated previously that long-term GDNF delivery results in TH downregulation and decreased DA uptake.[15]

In this study, the same dox-inducible vector was used to investigate the role of GDNF dose in nigrostriatal DA neurons survival and preservation of functionality in the 6-OHDA-induced rat PD model. We demonstrated that a sustained GDNF striatal concentration of ~200 pg/mg tissue (i.e., ~20-fold the endogenous level), after an initial improvement of motor function at 2 weeks post-vector injection, failed to halt motor deficit progression at later time points. In contrast, a 3- or 10-fold GDNF elevated level resulted in sustained motor symptoms. Consistent with the behavioral observations, in the 20-fold GDNF group, the number of VMAT2+ DA neurons was not increased and striatal DA innervation was impaired. Notwithstanding, in the 3- and 10-fold groups, DA neurons were preserved.

Since GDNF has been shown to increase dopamine concentration in the SNc[51] and striatum,[4,10] and given the dopamine oxidative properties[52,53] have been suggested to confer a selective vulnerability to DA neurons,[54,55] we measured the level of 8-oxo-dG, a commonly used marker of oxidative stress, in DA neurons. The main finding of this study is that animals with a 20-fold elevated striatal GDNF concentration showed increased 8-oxo-dG levels in the SNc. Hence, the sustained 20-fold GDNF dosage generating oxidative stress-mediated damage could have caused the loss of initial benefits. However, this was not the case for lower GDNF doses or intermittent treatment.

Oxidative DNA damage has been linked to neuronal cell death contributing to the disease progression.[56] Indeed, in patients with PD, the levels of 8-oxo-dG were significantly elevated in the SNc compared with those in age-matched controls.[57] However, further research is necessary to determine the potential role of 8-oxo-dG in PD pathogenesis. Nonetheless, our data are important for the design of future clinical trials using GDNF.

The need for close-to-physiological GDNF level to re-establish dopamine homeostasis and a controlled motor loop is not surprising. High-dose L-DOPA administration has also been suggested to be toxic due to conversion to excessive levels of dopamine, the self-oxidation and catabolism of which lead to the production of reactive oxygen species.[58–60] Strikingly, L-DOPA intraperitoneal administration to rats has been shown to generate 6-OHDA in the striatum.[61] Changes in oxidative stress and mitochondrial DNA copy numbers in patients with PD, particularly those undergoing long-term dopamine therapy, were reported, whereas there is evidence that moderate doses attenuate oxidative stress.[62] Whether L-DOPA could accelerate disease progression in patients by potentiating neuron death remains unanswered. Hence, it is recommended to use the lowest possible dose that compensates for the loss of dopamine.[63]

Nigrostriatal DA neurons consist of a highly complex and heterogeneous cell population. They differ in their morphological, molecular, and functional characteristics[64] and harbor a remarkably wide striatal arborization.[65] Neurons with an extensive field of terminals and large somata are under higher metabolic demands and mitochondrial activity and therefore more vulnerable to oxidative stress.[32–34,66] Accordingly, DA neurons surviving to degeneration in PD are smaller

Figure 5. Deleterious effects of long-term supraphysiological GDNF treatment

(A) Midbrain sections from the high-dose experiment were co-labeled with anti-8-oxo-dG antibodies revealed with a secondary antibody coupled to an Alexa Fluor 647 (red fluorescence) and an anti-VMAT2 antibody revealed with a secondary antibody coupled to an Alexa Fluor 488 (green fluorescence). The mean fluorescence intensity (MFI) per cell of the 8-oxo-dG labeling was measured on five sections per animal and three fields per section. MFI relative to the control group are shown. One-way ANOVA followed by Dunnett's multiple comparisons test. All groups were compared with the control group, i.e., GFP group pooled PBS group. Scale bars, 20 μm. (B) The area of VMAT2+ fibers in the SNr was measured on three sections per animal in both hemispheres. Means and SD of the percentage of injected (lesioned) side VMAT2+ area relative to the contralateral (intact) side are shown. One-way ANOVA followed by Dunnett's multiple comparisons test (all groups compared with the GFP group). Scale bars, 20 μm.

Table 1. Summary of beneficial and detrimental effects of different regimens of AAV-V16-mediated GDNF intrastriatal delivery

	Benefits				Deleterious effects	
hGDNF dose	Motor symptoms relief	DA neurons survival	DA neurons size	Striatal DA fibers	Oxidative stress	Aberrant sprouting
3×	+	+	+	+	–	–
10×	+	+	NT	NT	NT	NT
20×	–	–	–	–	+	+
20× Int.	+	+	–	+	–	–

The beneficial effects evaluated in this study were: motor symptoms relief, DA neuron survival and size, striatal DA innervation. Oxidative stress and aberrant sprouting were the deleterious effects considered in this study. +, effect present; –, effect absent; NT, not tested.

in size than in healthy humans.[67] A decrease of DA neuron mean size has also been observed in 6-OHDA-treated rats and MPTP-treated non-human primates.[35–37,67] Although some studies suggest that this may be due to the undergoing atrophy during the degenerative process, others indicate that large neurons are more vulnerable to 6-OHDA than small neurons. Interestingly, an increase in DA neuron size upon GDNF treatment in MPTP-lesioned monkeys has been reported previously.[37] In this study, the mean VMAT2+ cell area was higher in the GDNF 3× group compared with the control (lesioned but not GDNF-treated) group. In contrast, the GDNF 20× treatment did not increase the mean cell size. These data are in agreement with the increased level of oxidative damage in the 20× treatment group, which possibly preferentially affected large neurons.

In addition to high-dose GDNF-induced oxidative stress, herein reported for the first time, that a previously described adverse effect, i.e., aberrant sprouting,[29] is also in line with the importance of adjusting GDNF dose to avoid deleterious effects. Indeed, aberrant DA sprouting was observed in GDNF 20× but not GDNF 3× animals. This phenomenon, previously described using a lentiviral vector delivering high GDNF doses in the rat striatum,[29] was suggested to be caused by anterograde GDNF delivery in striatal efferent regions following AAV transduction of striatal projection neurons.[68]

Several authors have shown that low GDNF doses are sufficient to obtain therapeutically relevant biological effects.[10,14,28,69] To address safety aspects, i.e., the risks of tumorigenic potential[69] and adverse effects such as dyskinesia or anorexia,[23,70] others underline the need to regulate GDNF delivery.[13,71–73] However, it has never been demonstrated that, in addition, controlling GDNF dose is a requirement for efficient and sustained therapeutic effects. In our study, a side-to-side comparison of three different doses delivered in animals injected with the same AAV vector at the same time but treated with different inducer doses was performed. We show for the first time that high-dose GDNF, while providing faster symptomatic relief, becomes toxic, in the long-term resulting in the loss of benefits. Low-dose treatment provides slower but sustained symptomatic benefits.

Intermittent high-dose treatment also provided long-term symptomatic relief in the absence of oxidative stress but failed to fully restore a normal nigrostriatal DA pathway. Indeed, although these animals showed increased VMAT2+ neuronal survival, the mean cell area was not significantly restored. These results could be explained by compensatory mechanisms counterbalancing the protective GDNF effects in the GDNF 20× Int. group or different mechanisms conferring protection to the GDNF 3× and GDNF 20× Int. groups. It should be stressed that our intermittent treatment regimen consisted of 2 weeks dox administration interrupted by 2 weeks without treatment. It remains to be determined whether shorter treatments or longer interruptions as tested with the GeneSwitch study[13,74] could allow to restore the mean cell size.

Until now, promoters that do not allow for the control of transgene expression levels have been used in AAV-based GDNF clinical trials.[24]

Pharmacologically controlled viral vectors[13,75–77] raise the issue of the acceptability of a long-term drug treatment. Some systems have, however, been developed that use drugs at clinically acceptable doses.[28,71,78] In particular, the dox-inducible vector expressing hGDNF used in this study, allowed to obtain DA neuron protection and halt the progression of motor symptoms at a dox dose of 200 mg/kg dox diet, corresponding to a dox plasmatic concentration of 319 ± 50 ng/mL,[28] which is below the antimicrobial threshold (1 mg/mL) and in the range of doses used to treat benign inflammatory diseases such as rosacea or periodontitis, with no effect on intestinal[79] or subgingival[80,81] flora.

The other issue is immunogenicity of the bacterial elements present in the tetracycline transactivator.[82] Pre-clinical data suggest that, contrarily to peripheral administration,[82] brain[83] or retinal[84] tetracycline transactivator expression does not result in cellular immune responses nor in a decrease of transgene expression.

Another challenge will be to adapt the inducer dose to the patient's needs. The development of a sensitive ELISA allowing to evaluate GDNF concentration in the serum[85] could provide an interesting tool, associated with brain imaging and clinical evaluation.[23,24]

In conclusion, the way to neuroprotective gene therapy for PD patients is still paved with important challenges but increasing mechanistic knowledge and next-generation delivery tools will hopefully allow to optimize clinical benefits and safety. In this regard, the dox-inducible vector could allow to increase GDNF clinical benefits

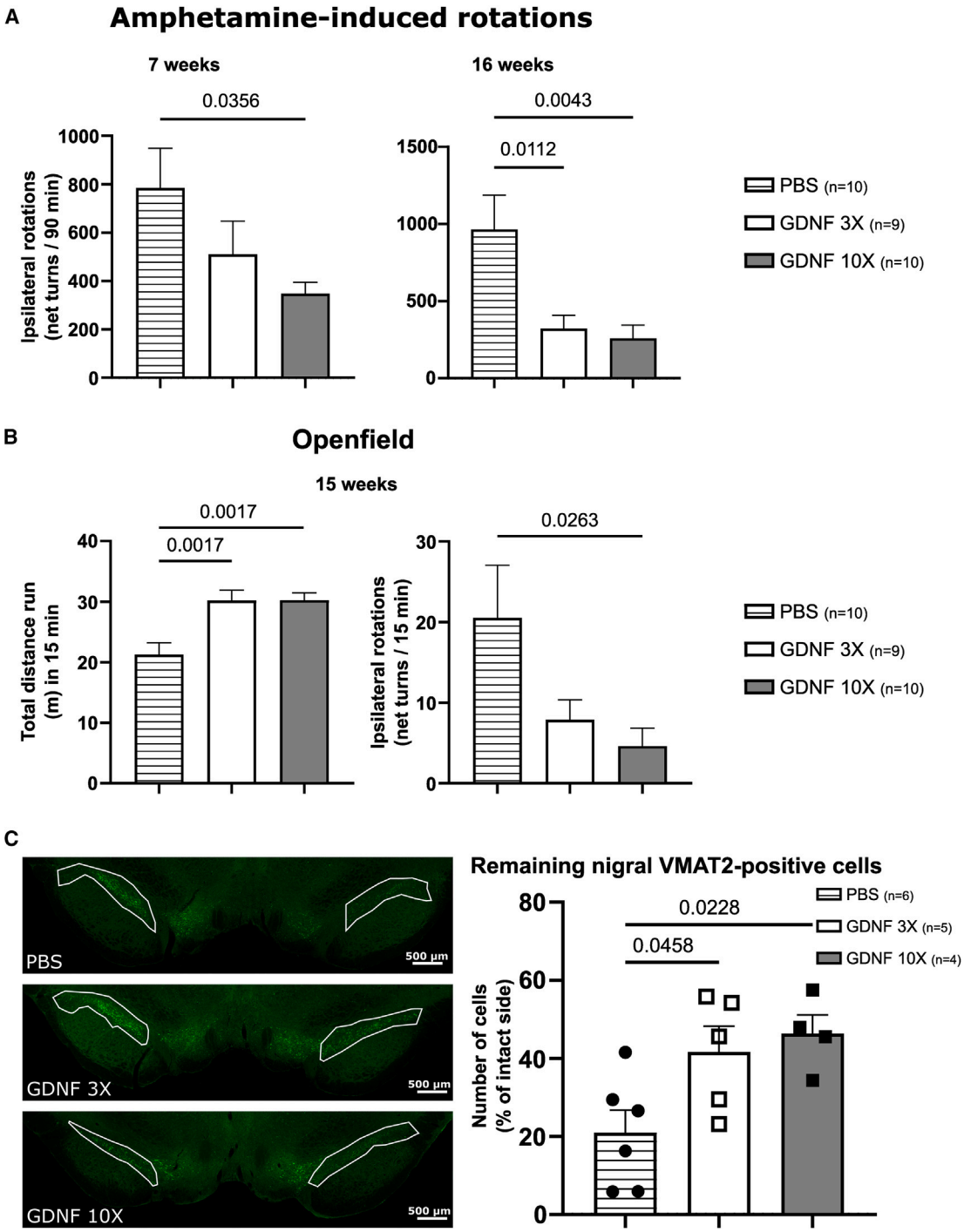

Figure 6. Sustained motor symptoms relief and dopaminergic neurons protection at moderate vector dose and clinically acceptable dox dose

(A) Correction of asymmetric amphetamine-induced rotational behavior. The animals from the low-dose experiment were injected intraperitoneally with amphetamine (2.5 mg/kg), harnessed to the rotameter, and the number of turns was measured using the Fusion software for 90 min. Statistical analysis was performed using one-way ANOVA followed by Dunnett's multiple comparisons test (all groups were compared with the PBS group). Means and SD are shown. (B) Motor behavior improvements in drug-free, free moving rats. Rats were placed in the middle of the open field and their movements were recorded during 15 min. Left panel: total distance run. Right panel: net number of ipsilateral turns. Statistical analysis was performed using one-way ANOVA followed by Dunnett's multiple comparisons test (all groups were compared with the

(legend continued on next page)

in the absence of adverse effects, provided the herein described GDNF dose toxicity threshold is considered. Furthermore, the toxic effects of high GDNF concentrations suggest that the viral particle injection method should ensure a homogeneous putamen coverage to avoid local over-dosage.

MATERIALS AND METHODS

Plasmids

The pAC1-V16 plasmid comprising AAV ITRs bracketing a bidirectional tetracycline-responsive cassette expressing the mutant dox-hypersensitive reverse tetracycline transactivator *rtTAV16*[86] and *eGFP* or human *GDNF* (*hGDNF*) cDNA (GenBank: AH003115.2) in the opposite direction, have been described previously[28] and were deposited at Addgene (www.addgene.org; plasmid no. 122035). The encapsidation plasmid encoding Rep proteins from AAV serotype 2 and capsid proteins from AAV serotype 5, pAAV2/5, was provided by the Penn Vector Core (Philadelphia, PA). The helper plasmid encoding adenoviral genes necessary for AAV replication and encapsidation, pAd-helper, was purchased from Stratagene (La Jolla, CA).

Cell lines

The HEK293T human embryonic kidney cell line was obtained from Q-One Biotech (Glasgow, UK). Cells were cultured in Dulbecco's modified Eagle's medium (DMEM) (Life Technologies) supplemented with 10% fetal bovine serum (FBS) (Sigma) and penicillin-streptomycin (InVitrogen). The 9L rat glioma cell line, a kind gift from Dr Catherine Bruyns,[87] was cultured in DMEM supplemented with 10% FBS and penicillin-streptomycin.

Recombinant AAV production

The viruses used in this study were produced by triple transfection of HEK293T cells using polyethylenimine (PEI) MW 25,000 (Polysciences, no. 23966-2). Thirty (10-cm) plates seeded with 5.0×10^6 cells per plate were transfected with the vector plasmids pAC1-V16-hGDNF or pAC1-V16-eGFP together with pAAV2/5 and pAd-helper in a 5:2:3 M ratio. Eleven micrograms of total DNA and 55 μg PEI were used per plate. Fifty hours post-transfection, cells were harvested by low-speed centrifugation, medium was discarded, and cells were resuspended in 50 mM Tris (pH 8.5), 0.1 M NaCl, and 1 mM EDTA, and kept at −20°C. After five freezing/thawing cycles at −20°C/37°C, the cell lysate was centrifuged for 20 min at 11,000 rpm. The supernatant was recovered and treated with benzonase (50 units/mL, Sigma) for 30 min at 37°C and centrifuged again for 20 min at 11,000 rpm to eliminate residual debris. The viruses were purified by iodixanol gradient followed by a QXL ion-exchange column (HiTrap QXL GE Healthcare, no. 17-5159-01) and microconcentrated as described previously.[88]

AAV vector titration

Quantification of viral genomes

Viral genomes (vg) were titrated by quantitative polymerase chain reaction as described previously[88] except that samples were treated with proteinase K (Life Technologies) at a concentration of 200 μg/mL for 30 min at 56°C prior to qPCR. Primers used were, respectively, universal primers located in the viral ITR sequences[89] for AAV2/5-V16-*eGFP* or GDNF primers: forward 5′-TGACTTGGGTCTGGGC TATGA-3′ and reverse 5′-AAGAGCCGCTGCAGTACCTAAA-3′ for AAV2/5-V16-*hGDNF*.

Titers were: AAV2/5-V16-*eGFP*, 3.8×10^{13} vg/mL; and AAV2/5-V16-*hGDNF*, $5.8 \pm 1.0 \times 10^{13}$ vg/mL (batch no. 1) and $5.0 \pm 1.7 \times 10^{13}$ vg/mL (batch no. 2). To match vector amounts of AAV batches, the quantification of viral genomes is not sufficient. Accurate titration requires a measurement of biologically active vector genomes, i.e., an infectious particles assay or a transgene expression assay.[90] For AAV2/5-V16-*hGDNF*, the functional titer defined as GDNF T.U. was evaluated by *in vitro* transduction assay on the 9L cell line (Table S1) and the amounts of vector injected were standardized accordingly for matching the titers between different experiments.

AAV2/5-V16-hGDNF functional titer

Ten thousand 9L rat gliosarcoma cells were seeded in 12-well plates (Nunc) and incubated in the presence of AAV2/5-V16-*hGDNF* at a multiplicity of infection of 1.0×10^5 vg/cell in serum-free DMEM for 2 h. After infection, the medium was replaced by DMEM supplemented with 10% FBS and dox (1 μg/mL). The medium was discarded 48 h later. Fresh dox-supplemented medium was added to the cells and collected after 1 h. GDNF content into the supernatant was quantified as described in the GDNF ELISA section (Promega kit). GDNF T.U. were defined as the amount of viral suspension producing 1 pg/mL GDNF *in vitro*.

Rats

The experiments were conducted on a total of 184 female Wistar rats (Janvier Labs, France) weighting approximately 200 g (7 weeks old). Twenty rats were used for the establishment of 6-OHDA injection parameters, 44 for the kinetics of AAV2/5-mediated GDNF expression, 88 for the high-dose experiments, and 32 for the low-dose experiments (Figure 1B).

All animal procedures were approved by the State Veterinary Office of Switzerland (authorization nos. VD3056 and VD3400).

Stereotaxy

Before stereotaxy, animals were anesthetized by intraperitoneal injection of a mixture of ketamine (100 mg/kg, Ketasol, Graeub AG) and

PBS group). Means and SD are shown. (C) Midbrain sections from the low-dose experiment were labeled with anti-VMAT2 antibodies revealed with a secondary antibody coupled to a green fluorophore. The total number of VMAT2+ cells were counted on the ipsilateral and contralateral SNc (delineated in white) on five sections per animal. The number of VMAT2-expressing cells in the ipsilateral SNpc relative to the contralateral side is shown for the three groups of rats from the low-dose experiment. Mean and SD are given. One-way ANOVA followed by Dunnett's multiple comparisons test. All groups were compared with the control PBS group. Scale bars, 500 μm.

xylasine (10 mg/kg, Rompun, Bayer) and placed in a Kopf stereotaxic frame (Kopf Instruments, Tujunga, CA). Injections were performed according to coordinates defined by the Paxinos and Watson rat brain atlas.[91]

Partial 6-OHDA model

To prevent destruction of noradrenergic neurons, desipramine (5 mg/kg, Sigma-Aldrich) was administered intraperitoneally 30 min prior to the infusion of 6-OHDA. Rats underwent an injection of 6-OHDA (10 or 15 μg; Sigma-Aldrich; calculated as a free base and dissolved in 0.9% saline with 0.05% ascorbic acid). One microliter was injected at a speed of 0.2 μL/min in each of the three or four delivery sites of into the right striatum. The three-site injections were performed along three different needle tracks: (1) anterioposterior (AP) = +1.0, mediolateral (ML) = −3.0, dorsoventral (DV) = −5.0; (2) AP = +0.1, ML = −3.7, DV = −5.0; (3) AP = −1.2, ML = −4.5, DV = −5.0. The four-site injections were performed along two different needle tracks, each with two different vertical coordinates: (1) AP = +1.0, ML = −3.6, DV = −4.0, and − 5.0 and (2) AP = +0.0, ML = −2.8, DV = −4.5 and −5.5, relative to the bregma and the dural surface.

AAV vector injections

Viral particles diluted in 1 μL of D-PBS (Biowhittaker, Lonza) were infused in the right striatum using a 34G needle. The injection coordinates were the same as for the four-site 6-OHDA injection. Vector deposits were made at two different positions along two injection tracks at 4.5 and 5.5mm below the dural surface. The needle was first carefully lowered to the lowest level and left in place for 5 min before starting the injection. One microliter of vector was injected at each injection site at a rate of 0.2 μL/min. At the end of the injection, the needle was left in place for 5 min before being slowly moved to the next injection coordinate.

When indicated, rats were fed with dox-supplemented food (Dox diet, Safe, France) at the indicated dose. The food was replaced every second day to keep a stable dox concentration. At the end of the experiment, euthanasia was performed using pentobarbital injection at a dose of 300 mg/kg.

FG injections

For retrograde tracing of the nigrostriatal pathway, 1 μL of a FG (FluoroChrome, Denver, CO) solution (1.5% in saline) was infused in the right striatum in four sites at the same coordinates as for 6-OHDA. Animals were euthanized 2 weeks after injection.

Behavior

Amphetamine-induced rotation test

Rats were harnessed and connected to automated rotameter bowls (AccuScan Instruments, OH.). D-Amphetamine sulfate (2.5 mg/kg; Lipomed AG, Switzerland) was injected intraperitoneally and rotational asymmetry was recorded over 90 min. Mean net rotations are expressed as full body turns (ipsilateral minus contralateral to the lesion) per 90 min.

Open-field tests

The animals were placed in a circular arena (70 cm diameter and 23 lux illumination). Total distance run and the number of full rotations during 15 min were evaluated using the ANY-maze software.

The experiments were performed in an experimenter-blinded manner.

Immunohistochemistry

At the end of the experiments, euthanasia was performed using pentobarbital (in 0.9% NaCl) injection at a dose of 300 mg/kg. Animals were perfused transcardially with 100 mL of PBS (pH 7.4) followed by 200 mL of ice-cold 4% paraformaldehyde (PF4) in PBS pH 7.4. After overnight post-fixation in PF4 at 4°C, brains were transferred successively to sucrose 20% and 30% at 4°C, gradually frozen by consecutive immersion in 2-methyl-butane/dry ice bath at −10°C and −20°C and subsequently stored at −80°C. Cryostat (Leica Biosystems, CM1850) 40-μm-thick coronal sections were stored in an anti-freeze solution (25% glycerol, 30% ethylene glycol, and 50 mM Na-phosphate buffer) at −20°C. For chromogenic immunostainings, free-floating sections were sequentially incubated for 30 min in 3% H_2O_2 and 10% methanol in TBS (10 mmol/L Tris, 0.9% NaCl [pH 7.6]), then for 1 h in THST (50 mmol/L Tris, 0.5 M NaCl, 0.5% Triton X-100 [pH 7.6]) containing 5% bovine serum albumin (BSA) (Sigma) and overnight at 4°C with the primary antibody diluted in THST containing 1% BSA. After washing, slices were incubated with a biotinylated secondary antibody during 1 h at room temperature (RT). The peroxidase staining was revealed with a VECTASTAIN Elite ABC kit and diaminobenzidine (Vector Laboratories, Burlingame, CA) according to the manufacturer's protocol. Sections were mounted on slides, dehydrated, and overlaid with Eukitt mounting fluid (Sigma-Aldrich).

For TH immunostaining, the primary antibody was a mouse monoclonal anti-TH (dilution 1:500, Chemicon, Temecula, CA, cat. no. MAB 318) and the secondary antibody was a biotinylated anti-mouse antibody (1:400, BD Pharmingen, cat. no. Bd553441). For GDNF immunostaining, sections were first incubated for 10 min in 10 mM Na citrate buffer, 0.05% Tween 20 (pH 6.0) on a hot plate at 65°C for heat-induced antigen retrieval and then cooled down for 5 min. The sections were washed in TBS and endogenous peroxidase was blocked as described above. Sections were incubated overnight at 4°C with a goat anti-GDNF primary antibody (dilution 1:500, R&D Systems, cat. no. BAF212) followed by a biotinylated donkey anti-goat secondary antibody (dilution 1:600, Jackson Laboratories, cat. no. 105605).

Images were acquired using a Zeiss Axioscan Z1, at a 10× magnification, 0.45 of numeric aperture, and were saved as TIFF files using Zen 2 Software (CIF facility of the Lausanne University, Bugnon). TH+ cell countings were performed at AP = −5.30 of the SNpc for each individual, using Fiji (ImageJ) software. For TH and VMAT2 striatal labeling, gray level quantifications were performed on four to six sections for each individual, using Fiji software.

Immunofluorescence

Free-floating sections obtained and stored as for immunohistochemistry, were stained as follows. Sections were washed 3 times for 10 min in TBS at RT, then incubated for 1 h at RT in a blocking solution composed of 5% BSA in THST buffer. Afterward, they were incubated overnight at 4°C with the primary antibody in THST containing 1% BSA. On the second day, sections were first washed 3 times for 10 min in TBS at RT and then incubated for 1 h at RT with the secondary antibody in THST. Sections were then washed 3 times for 10 min in TBS and incubated in the dark with the streptavidin conjugate for 1 h at RT in THST. Finally, the sections were washed 3 times in PBS for 10 min at RT, mounted on microscope slides, and covered with Vectashield mounting medium (Vector Laboratories).

Primary antibodies were: rabbit anti-VMAT2 (1:500, Synaptic Systems, cat. no. 138,302), and mouse anti-8-oxo-dG (1:300, Travigen, cat. no. 4353-mc-050). Secondary antibodies were: Alexa Fluor 647 donkey-anti mouse IgG (1:500, Molecular Probes cat. no. A-31571) and Cy3 donkey anti-rabbit IgG (1:500, Jackson Laboratories, cat. no. 711-165-152).

Image acquisition and quantifications

Whole-slide images were taken with a Zeiss Axioscan Z.1 (Carl Zeiss Microscopy, Germany) using a Plan-Apochromat 10×/0.45 or a Plan-Apochromat 20×/0.8 objective and using an Orca-Flash 4.0 V2 digital CMOS camera. Cy3 was excited at 553 nm with 555/30 nm LED at 50% power. A beam splitter at 568 nm was used. The detection range was 578–640 nm. Alexa Fluor 488 was excited at 493 nm with a 469/38 nm LED at 20% of power. A beam splitter at 498 nm was used. The detection range was 507–545 nm. For chromogenic immunostaining, the bright-field contrast method was used with 206% light source intensity. Sixteen-bit images were obtained, processed, and exported as .tiff files using Zen Blue 2.3 (Carl Zeiss Microscopy). They were then analyzed using Fiji software (https://doi.org/10.1038/nmeth.2019). The "Cell Counter" tool was used to manually count the number of cells. To quantify the mean fluorescence intensity, regions of interest were manually defined and the fluorescence intensity was measured using the "ROI manager" tool.

Confocal images were taken with a Zeiss LSM 800 confocal microscope (Carl Zeiss Microscopy) equipped with a 3× GaAsp detector and using a 20×/0.8 DIC II objective with a pinhole set at 31 μm. Alexa Fluor 488 was excited with a 488 nm laser at 0.10% of power. A master gain of 650 V was applied and the detection range was 400–592 nm. Alexa Fluor 647 was excited with a 640 nm laser at 1.30% of power. A master gain of 800 V was applied and the detection range was 657–700 nm. For FG, z stacks of 66 slices covering 31.85 μm of tissue depth were made by directional scanning and 4× averaging. The slice overlap was at least 50% for both channels. The resulting 8-bit images ".czi" format files were processed using Fiji.

TH+, VMAT2+, and FG+ cells, as well as TH+/FG+, VMAT2+/FG+, and TH+/VMAT2+ double-labeled cells, were manually counted on confocal images in a double-blinded manner. For each animal, five brain sections were selected and three pictures were taken for each section. Quantification of the fluorescence intensity of individual cells was performed using Fiji software. In brief, maximum intensity projections were performed, and the channels were split. Then, the channel of interest was duplicated, background noise reduction was performed using the function "Subtract background" (rolling = 100), and the image was converted to a mask. The function "Analyze Particles" (size 100–1,000 μm^2) was used to recognize the cells and add them to the "ROI Manager." Finally, the measure option of ROI Manager was used to measure the mean fluorescence intensity and cell area.

To quantify the VMAT2+ innervation of the SNr, confocal images of the medial part of SNr were taken using the parameters described above. Maximum intensity projections were performed using Fiji software. Substract background (rolling = 100) was used. The function Analyze Particles (size 1-Infinity) was used to recognize the nigral VMAT2+ signal. Finally, the measure option of ROI Manager was used to measure the area in μm^2 covered by VMAT2+ signal.

Western blotting

Animals were euthanized with a pentobarbital overdose (30 mg/mL in 0.9% NaCl, Esconarkon) and then decapitated. After decapitation, brains were removed and dissected on ice using stainless-steel brain matrix (Stoelting) and single-edge blades. For the preparation of the tissue extract, small pieces of striatum were triturated in Tissue Protein Extraction Reagent (T-per) (Thermo Scientific) supplemented with protease inhibitor cocktail (Roche) and anti-phosphatases (Roche). Samples were centrifuged at 10,000 × *g* at 4°C (10 min) and supernatants were harvested. Proteins were quantified using the bicinchoninic acid (Sigma) method and BSA (Panreac, Barcelona, Spain) as standard. Protein samples were diluted in Laemmli's loading buffer (62.5 mM Tris-HCl, 20% glycerol [Sigma], 2% sodium dodecyl sulfate [SDS, Sigma], 1.7% β-mercaptoethanol [Sigma], and 0.05% bromophenol blue [Sigma, pH 6.8]), denatured (90°C, 5 min), separated by electrophoresis in 10% SDS-polyacrylamide gel, and transferred to nitrocellulose (Schleicher & Schuell, Dassel, Germany). Blots were blocked for 2 h at RT with 5% non-fat dry milk, and incubated overnight at 4°C in blocking solution with rabbit polyclonal anti-VMAT2 (1:1,000, Merck, Darmstadt, Germany) or mouse monoclonal anti-TH (1:30,000, Sigma). After several rinses in TBST-5% milk, the membranes were incubated for 1 h in peroxidase-conjugated anti-rabbit-IgG (1:50,000, Jackson Immunoresearch) or peroxidase-conjugated anti-mouse-IgG (1:50,000, Jackson Immunoresearch). After processing, each nitrocellulose membrane was reblotted for the sample loading marker β-actin (1:50,000, Sigma). The anti-VMAT2 antibody detects two bands, one at 62 kDa and another at 80 kDa, which correspond to the non-glycosylated form and a glycosylated form of the transporter, respectively.[92,93] Each TH and VMAT2 immunoreactive band was compared with its loading control. Different protein quantities, antibody dilutions, and exposure times were tested to establish their working range. Immunoreactive bands were visualized using enhanced chemiluminescence (Immun-Star, Bio-Rad, CA) and a

Chemi-Doc imaging system (Bio-Rad). The labeling densities were quantified using a densitometry software (Image Lab 5.2; Bio-Rad). A rectangle of uniform size and shape was placed over each band, and the density values were calculated by subtracting the background at approximately 2 mm above each band. The origin of protein extract was blinded for the quantitative analysis of western blot images. Data are expressed as a percentage of the mean labeling intensity in basal conditions ± SEM.

GDNF ELISA

For determination of GDNF brain tissue levels, protein extracts were prepared as for western blotting. GDNF striatal concentrations were evaluated using the GDNF Emax ImmunoAssay System (Promega) ELISA kit, which equally detects rat and human GDNF (high-dose experiment) or the DuoSet "Human GDNF Elisa" kit (R&D Systems), which poorly detects rat GDNF (low-dose experiment), according to the manufacturer's protocol. Recombinant human GDNF (provided by the manufacturer) was used to establish the standard curve. Cross-reactivity with mouse[14] and rat GDNF[94] was 100% for the Promega kit. With the R&D Systems kit, the cross-reactivity for rat GDNF is low.

The GDNF concentrations were expressed as pg/mg tissue. For determination of GDNF in cell culture medium, supernatants were harvested. GDNF concentrations were measured using the Promega kit and expressed in pg/mL. A comparison between the Promega GDNF Emax ImmunoAssay System and the R&D Systems Human DuoSet GDNF ELISA has been performed and similar values of hGDNF concentration in striatal tissue injected with AAV2/5-V16-hGDNF were obtained (data not shown).

Statistical analysis

After confirmation of normality, analyses were performed using one-way ANOVA followed by Dunnett's multiple comparison test.

DATA AND CODE AVAILABILITY

All data from this study are available in the main text, supplemental files, or from the corresponding author upon reasonable request.

SUPPLEMENTAL INFORMATION

Supplemental information can be found online at https://doi.org/10.1016/j.omtm.2023.09.002.

ACKNOWLEDGMENTS

We thank Pascal Steullet (Center for Neuropsychiatric Research, CHUV) as well as Pavlina Konstantinova, Bas Blits, and Harald Petry (UniQure) for helpful discussions. We thank Ali Scherz for technical help and Romain-Daniel Gosselin (Precision Medicine Unit, CHUV) for his help in statistical analyses. We thank Abdelwahed Chtarto (Free University of Brussels) for the gift of the AAV-V16 plasmids, Atze Das (Amsterdam Medical Center) for the gift of the V16 transactivator, and Jolanda Liefhebber (UniQure) for sharing the sequence of GDNF primers for vector titration. Scanning and confocal imaging were performed in CIF Lausanne University imaging platform. We particularly thank Luigi Bozzo and Florence Morgenthaler-Grand. The rats were housed and fed with dox diet when indicated at the Center for the Study of Behavior at the Center for Neuropsychiatric Research, CHUV. This work was supported by a grant from the Swiss National Foundation (SNF grant no. 31003A_179527) to L.T., by EU FP7 Marie Curie IAPP BrainVectors (contract no. 286071) to L.T., by UniQure to L.T. and M.H.-C., and by the "Spanish Ministry of Sciences and Innovation (PID2019-105795RB-I00)" to T.G.-H. The authors declare that there are no additional disclosures to report.

AUTHOR CONTRIBUTIONS

M.D.A., N.P., M.H.-C., V.M.-I., C.J., V.G., K.D.M., and B.B.J. conducted the experiments. M.D.A., N.P., M.H.-C., T.G.-H., F.M., and L.T. designed the experiments. M.D.A., L.T., and T.G.H. wrote the paper.

DECLARATION OF INTERESTS

The authors declare no competing interests.

REFERENCES

1. Kirik, D., Rosenblad, C., Bjorklund, A., and Mandel, R.J. (2000). Long-term rAAV-mediated gene transfer of GDNF in the rat Parkinson's model: intrastriatal but not intranigral transduction promotes functional regeneration in the lesioned nigrostriatal system. J. Neurosci. *20*, 4686–4700.
2. Kordower, J.H., Emborg, M.E., Bloch, J., Ma, S.Y., Chu, Y., Leventhal, L., McBride, J., Chen, E.Y., Palfi, S., Roitberg, B.Z., et al. (2000). Neurodegeneration prevented by lentiviral vector delivery of GDNF in primate models of Parkinson's disease. Science *290*, 767–773.
3. Kells, A.P., Eberling, J., Su, X., Pivirotto, P., Bringas, J., Hadaczek, P., Narrow, W.C., Bowers, W.J., Federoff, H.J., Forsayeth, J., and Bankiewicz, K.S. (2010). Regeneration of the MPTP-lesioned dopaminergic system after convection-enhanced delivery of AAV2-GDNF. J. Neurosci. *30*, 9567–9577. https://doi.org/10.1523/JNEUROSCI.0942-10.2010.
4. Yang, X., Mertens, B., Lehtonen, E., Vercammen, L., Bockstael, O., Chtarto, A., Levivier, M., Brotchi, J., Michotte, Y., Baekelandt, V., et al. (2009). Reversible neurochemical changes mediated by delayed intrastriatal glial cell line-derived neurotrophic factor gene delivery in a partial Parkinson's disease rat model. J. Gene Med. *11*, 899–912. https://doi.org/10.1002/jgm.1377.
5. Yang, F., Feng, L., Zheng, F., Johnson, S.W., Du, J., Shen, L., Wu, C.P., and Lu, B. (2001). GDNF acutely modulates excitability and A-type K(+) channels in midbrain dopaminergic neurons. Nat. Neurosci. *4*, 1071–1078. https://doi.org/10.1038/nn734.
6. Hebert, M.A., Van Horne, C.G., Hoffer, B.J., and Gerhardt, G.A. (1996). Functional effects of GDNF in normal rat striatum: presynaptic studies using *in vivo* electrochemistry and microdialysis. J. Pharmacol. Exp. Therapeut. *279*, 1181–1190.
7. Bourque, M.J., and Trudeau, L.E. (2000). GDNF enhances the synaptic efficacy of dopaminergic neurons in culture. Eur. J. Neurosci. *12*, 3172–3180.
8. Wang, J., Chen, G., Lu, B., and Wu, C.P. (2003). GDNF acutely potentiates Ca2+ channels and excitatory synaptic transmission in midbrain dopaminergic neurons. Neurosignals *12*, 78–88. https://doi.org/10.1159/000071817.
9. Salvatore, M.F., Zhang, J.L., Large, D.M., Wilson, P.E., Gash, C.R., Thomas, T.C., Haycock, J.W., Bing, G., Stanford, J.A., Gash, D.M., and Gerhardt, G.A. (2004). Striatal GDNF administration increases tyrosine hydroxylase phosphorylation in the rat striatum and substantia nigra. J. Neurochem. *90*, 245–254. https://doi.org/10.1111/j.1471-4159.2004.02496.x.
10. Eslamboli, A., Georgievska, B., Ridley, R.M., Baker, H.F., Muzyczka, N., Burger, C., Mandel, R.J., Annett, L., and Kirik, D. (2005). Continuous low-level glial cell line-derived neurotrophic factor delivery using recombinant adeno-associated viral vectors provides neuroprotection and induces behavioral recovery in a primate model of Parkinson's disease. J. Neurosci. *25*, 769–777. https://doi.org/10.1523/JNEUROSCI.4421-04.2005.

11. Rosenblad, C., Georgievska, B., and Kirik, D. (2003). Long-term striatal overexpression of GDNF selectively downregulates tyrosine hydroxylase in the intact nigrostriatal dopamine system. Eur. J. Neurosci. *17*, 260–270.

12. Georgievska, B., Kirik, D., and Björklund, A. (2004). Overexpression of glial cell line-derived neurotrophic factor using a lentiviral vector induces time- and dose-dependent downregulation of tyrosine hydroxylase in the intact nigrostriatal dopamine system. J. Neurosci. *24*, 6437–6445. https://doi.org/10.1523/JNEUROSCI.1122-04.2004.

13. Tereshchenko, J., Maddalena, A., Bähr, M., and Kügler, S. (2014). Pharmacologically controlled, discontinuous GDNF gene therapy restores motor function in a rat model of Parkinson's disease. Neurobiol. Dis. *65*, 35–42. https://doi.org/10.1016/j.nbd.2014.01.009.

14. Kumar, A., Kopra, J., Varendi, K., Porokuokka, L.L., Panhelainen, A., Kuure, S., Marshall, P., Karalija, N., Härma, M.A., Vilenius, C., et al. (2015). GDNF Overexpression from the Native Locus Reveals its Role in the Nigrostriatal Dopaminergic System Function. PLoS Genet. *11*, e1005710. https://doi.org/10.1371/journal.pgen.1005710.

15. Barroso-Chinea, P., Cruz-Muros, I., Afonso-Oramas, D., Castro-Hernández, J., Salas-Hernández, J., Chtarto, A., Luis-Ravelo, D., Humbert-Claude, M., Tenenbaum, L., and González-Hernández, T. (2016). Long-term controlled GDNF over-expression reduces dopamine transporter activity without affecting tyrosine hydroxylase expression in the rat mesostriatal system. Neurobiol. Dis. *88*, 44–54. https://doi.org/10.1016/j.nbd.2016.01.002.

16. Lohr, K.M., Masoud, S.T., Salahpour, A., and Miller, G.W. (2017). Membrane transporters as mediators of synaptic dopamine dynamics: implications for disease. Eur. J. Neurosci. *45*, 20–33. https://doi.org/10.1111/ejn.13357.

17. Chu, Y., and Kordower, J.H. (2021). GDNF signaling in subjects with minimal motor deficits and Parkinson's disease. Neurobiol. Dis. *153*, 105298. https://doi.org/10.1016/j.nbd.2021.105298.

18. Mesa-Infante, V., Afonso-Oramas, D., Salas-Hernández, J., Rodríguez-Núñez, J., and Barroso-Chinea, P. (2022). Long-term exposure to GDNF induces dephosphorylation of Ret, AKT, and ERK1/2, and is ineffective at protecting midbrain dopaminergic neurons in cellular models of Parkinson's disease. Mol. Cell. Neurosci. *118*, 103684. https://doi.org/10.1016/j.mcn.2021.103684.

19. Marks, W.J., Jr., Bartus, R.T., Siffert, J., Davis, C.S., Lozano, A., Boulis, N., Vitek, J., Stacy, M., Turner, D., Verhagen, L., et al. (2010). Gene delivery of AAV2-neurturin for Parkinson's disease: a double-blind, randomised, controlled trial. Lancet Neurol. *9*, 1164–1172. https://doi.org/10.1016/S1474-4422(10)70254-4.

20. Lang, A.E., Gill, S., Patel, N.K., Lozano, A., Nutt, J.G., Penn, R., Brooks, D.J., Hotton, G., Moro, E., Heywood, P., et al. (2006). Randomized controlled trial of intraputamenal glial cell line-derived neurotrophic factor infusion in Parkinson disease. Ann. Neurol. *59*, 459–466. https://doi.org/10.1002/ana.20737.

21. Gill, S.S., Patel, N.K., Hotton, G.R., O'Sullivan, K., McCarter, R., Bunnage, M., Brooks, D.J., Svendsen, C.N., and Heywood, P. (2003). Direct brain infusion of glial cell line-derived neurotrophic factor in Parkinson disease. Nat. Med. *9*, 589–595. https://doi.org/10.1038/nm850.

22. Slevin, J.T., Gerhardt, G.A., Smith, C.D., Gash, D.M., Kryscio, R., and Young, B. (2005). Improvement of bilateral motor functions in patients with Parkinson disease through the unilateral intraputaminal infusion of glial cell line-derived neurotrophic factor. J. Neurosurg. *102*, 216–222. https://doi.org/10.3171/jns.2005.102.2.0216.

23. Whone, A., Luz, M., Boca, M., Woolley, M., Mooney, L., Dharia, S., Broadfoot, J., Cronin, D., Schroers, C., Barua, N.U., et al. (2019). Randomized trial of intermittent intraputamenal glial cell line-derived neurotrophic factor in Parkinson's disease. Brain *142*, 512–525. https://doi.org/10.1093/brain/awz023.

24. Heiss, J.D., Lungu, C., Hammoud, D.A., Herscovitch, P., Ehrlich, D.J., Argersinger, D.P., Sinharay, S., Scott, G., Wu, T., Federoff, H.J., et al. (2019). Trial of magnetic resonance-guided putaminal gene therapy for advanced Parkinson's disease. Mov. Disord. *34*, 1073–1078. https://doi.org/10.1002/mds.27724.

25. Bartus, R.T., Herzog, C.D., Chu, Y., Wilson, A., Brown, L., Siffert, J., Johnson, E.M., Jr., Olanow, C.W., Mufson, E.J., and Kordower, J.H. (2011). Bioactivity of AAV2-neurturin gene therapy (CERE-120): differences between Parkinson's disease and nonhuman primate brains. Mov. Disord. *26*, 27–36. https://doi.org/10.1002/mds.23442.

26. Bartus, R.T., Kordower, J.H., Johnson, E.M., Jr., Brown, L., Kruegel, B.R., Chu, Y., Baumann, T.L., Lang, A.E., Olanow, C.W., and Herzog, C.D. (2015). Post-mortem assessment of the short and long-term effects of the trophic factor neurturin in patients with alpha-synucleinopathies. Neurobiol. Dis. *78*, 162–171. https://doi.org/10.1016/j.nbd.2015.03.023.

27. Chu, Y., Bartus, R.T., Manfredsson, F.P., Olanow, C.W., and Kordower, J.H. (2020). Long-term post-mortem studies following neurturin gene therapy in patients with advanced Parkinson's disease. Brain *143*, 960–975. https://doi.org/10.1093/brain/awaa020.

28. Chtarto, A., Humbert-Claude, M., Bockstael, O., Das, A.T., Boutry, S., Breger, L.S., Klaver, B., Melas, C., Barroso-Chinea, P., Gonzalez-Hernandez, T., et al. (2016). A regulatable AAV vector mediating GDNF biological effects at clinically-approved sub-antimicrobial doxycycline doses. Mol. Ther. Methods Clin. Dev. *5*, 16027. https://doi.org/10.1038/mtm.2016.27.

29. Georgievska, B., Kirik, D., and Björklund, A. (2002). Aberrant sprouting and downregulation of tyrosine hydroxylase in lesioned nigrostriatal dopamine neurons induced by long-lasting overexpression of glial cell line derived neurotrophic factor in the striatum by lentiviral gene transfer. Exp. Neurol. *177*, 461–474.

30. Kirik, D., Rosenblad, C., and Björklund, A. (1998). Characterization of behavioral and neurodegenerative changes following partial lesions of the nigrostriatal dopamine system induced by intrastriatal 6-hydroxydopamine in the rat. Exp. Neurol. *152*, 259–277. https://doi.org/10.1006/exnr.1998.6848.

31. Penttinen, A.M., Suleymanova, I., Albert, K., Anttila, J., Voutilainen, M.H., and Airavaara, M. (2016). Characterization of a new low-dose 6-hydroxydopamine model of Parkinson's disease in rat. J. Neurosci. Res. *94*, 318–328. https://doi.org/10.1002/jnr.23708.

32. Bolam, J.P., and Pissadaki, E.K. (2012). Living on the edge with too many mouths to feed: why dopamine neurons die. Mov. Disord. *27*, 1478–1483. https://doi.org/10.1002/mds.25135.

33. Giguère, N., Burke Nanni, S., and Trudeau, L.E. (2018). On Cell Loss and Selective Vulnerability of Neuronal Populations in Parkinson's Disease. Front. Neurol. *9*, 455. https://doi.org/10.3389/fneur.2018.00455.

34. Wong, Y.C., Luk, K., Purtell, K., Burke Nanni, S., Stoessl, A.J., Trudeau, L.E., Yue, Z., Krainc, D., Oertel, W., Obeso, J.A., and Volpicelli-Daley, L.A. (2019). Neuronal vulnerability in Parkinson disease: Should the focus be on axons and synaptic terminals? Movement disorders. Mov. Disord. *34*, 1406–1422. https://doi.org/10.1002/mds.27823.

35. Rodríguez, M., Barroso-Chinea, P., Abdala, P., Obeso, J., and González-Hernández, T. (2001). Dopamine cell degeneration induced by intraventricular administration of 6-hydroxydopamine in the rat: similarities with cell loss in parkinson's disease. Exp. Neurol. *169*, 163–181. https://doi.org/10.1006/exnr.2000.7624.

36. Healy-Stoffel, M., Omar Ahmad, S., Stanford, J.A., and Levant, B. (2014). Differential effects of intrastriatal 6-hydroxydopamine on cell number and morphology in midbrain dopaminergic subregions of the rat. Brain Res. *1574*, 113–119. https://doi.org/10.1016/j.brainres.2014.05.045.

37. Grondin, R., Zhang, Z., Yi, A., Cass, W.A., Maswood, N., Andersen, A.H., Elsberry, D.D., Klein, M.C., Gerhardt, G.A., and Gash, D.M. (2002). Chronic, controlled GDNF infusion promotes structural and functional recovery in advanced parkinsonian monkeys. Brain *125*, 2191–2201. https://doi.org/10.1093/brain/awf234.

38. Nair, A., Morsy, M.A., and Jacob, S. (2018). Dose translation between laboratory animals and human in preclinical and clinical phases of drug development. Drug Dev. Res. *79*, 373–382. https://doi.org/10.1002/ddr.21461.

39. McKeage, K., and Deeks, E.D. (2010). Doxycycline 40 mg capsules (30 mg immediate-release/10 mg delayed-release beads): anti-inflammatory dose in rosacea. Am. J. Clin. Dermatol. *11*, 217–222. https://doi.org/10.2165/11204850-000000000-00000.

40. Del Rosso, J.Q., Webster, G.F., Jackson, M., Rendon, M., Rich, P., Torok, H., and Bradshaw, M. (2007). Two randomized phase III clinical trials evaluating anti-inflammatory dose doxycycline (40-mg doxycycline, USP capsules) administered once daily for treatment of rosacea. J. Am. Acad. Dermatol. *56*, 791–802. https://doi.org/10.1016/j.jaad.2006.11.021.

41. Lin, L.F., Doherty, D.H., Lile, J.D., Bektesh, S., and Collins, F. (1993). GDNF: a glial cell line-derived neurotrophic factor for midbrain dopaminergic neurons. Science *260*, 1130–1132. https://doi.org/10.1126/science.8493557.

42. Domanskyi, A., Saarma, M., and Airavaara, M. (2015). Prospects of Neurotrophic Factors for Parkinson's Disease: Comparison of Protein and Gene Therapy. Hum. Gene Ther. *26*, 550–559. https://doi.org/10.1089/hum.2015.065.

43. Eggers, R., de Winter, F., Tannemaat, M.R., Malessy, M.J.A., and Verhaagen, J. (2020). GDNF Gene Therapy to Repair the Injured Peripheral Nerve. Front. Bioeng. Biotechnol. *8*, 583184. https://doi.org/10.3389/fbioe.2020.583184.

44. Patel, N.K., Bunnage, M., Plaha, P., Svendsen, C.N., Heywood, P., and Gill, S.S. (2005). Intraputamenal infusion of glial cell line-derived neurotrophic factor in PD: a two-year outcome study. Ann. Neurol. *57*, 298–302. https://doi.org/10.1002/ana.20374.

45. Patel, N.K., and Gill, S.S. (2007). GDNF delivery for Parkinson's disease. Acta Neurochir. Suppl. *97*, 135–154. https://doi.org/10.1007/978-3-211-33081-4_16.

46. Slevin, J.T., Gash, D.M., Smith, C.D., Gerhardt, G.A., Kryscio, R., Chebrolu, H., Walton, A., Wagner, R., and Young, A.B. (2007). Unilateral intraputamenal glial cell line-derived neurotrophic factor in patients with Parkinson disease: response to 1 year of treatment and 1 year of withdrawal. J. Neurosurg. *106*, 614–620. https://doi.org/10.3171/jns.2007.106.4.614.

47. Love, S., Plaha, P., Patel, N.K., Hotton, G.R., Brooks, D.J., and Gill, S.S. (2005). Glial cell line-derived neurotrophic factor induces neuronal sprouting in human brain. Nat. Med. *11*, 703–704. https://doi.org/10.1038/nm0705-703.

48. Gash, D.M., Gerhardt, G.A., Bradley, L.H., Wagner, R., and Slevin, J.T. (2020). GDNF clinical trials for Parkinson's disease: a critical human dimension. Cell Tissue Res. *382*, 65–70. https://doi.org/10.1007/s00441-020-03269-8.

49. Van Laar, A.D., Van Laar, V.S., San Sebastian, W., Merola, A., Elder, J.B., Lonser, R.R., and Bankiewicz, K.S. (2021). An Update on Gene Therapy Approaches for Parkinson's Disease: Restoration of Dopaminergic Function. J. Parkinsons Dis. *11*, S173–S182. https://doi.org/10.3233/JPD-212724.

50. Kopra, J.J., Panhelainen, A., Af Bjerkén, S., Porokuokka, L.L., Varendi, K., Olfat, S., Montonen, H., Piepponen, T.P., Saarma, M., and Andressoo, J.O. (2017). Dampened Amphetamine-Stimulated Behavior and Altered Dopamine Transporter Function in the Absence of Brain GDNF. J. Neurosci. *37*, 1581–1590. https://doi.org/10.1523/JNEUROSCI.1673-16.2016.

51. Smith, M.P., and Cass, W.A. (2007). GDNF reduces oxidative stress in a 6-hydroxydopamine model of Parkinson's disease. Neurosci. Lett. *412*, 259–263. https://doi.org/10.1016/j.neulet.2006.11.017.

52. Schildknecht, S., Gerding, H.R., Karreman, C., Drescher, M., Lashuel, H.A., Outeiro, T.F., Di Monte, D.A., and Leist, M. (2013). Oxidative and nitrative alpha-synuclein modifications and proteostatic stress: implications for disease mechanisms and interventions in synucleinopathies. J. Neurochem. *125*, 491–511. https://doi.org/10.1111/jnc.12226.

53. Fahn, S., and Cohen, G. (1992). The oxidant stress hypothesis in Parkinson's disease: evidence supporting it. Ann. Neurol. *32*, 804–812. https://doi.org/10.1002/ana.410320616.

54. Ni, A., and Ernst, C. (2022). Evidence That Substantia Nigra Pars Compacta Dopaminergic Neurons Are Selectively Vulnerable to Oxidative Stress Because They Are Highly Metabolically Active. Front. Cell. Neurosci. *16*, 826193. https://doi.org/10.3389/fncel.2022.826193.

55. Lohr, K.M., Bernstein, A.I., Stout, K.A., Dunn, A.R., Lazo, C.R., Alter, S.P., Wang, M., Li, Y., Fan, X., Hess, E.J., et al. (2014). Increased vesicular monoamine transporter enhances dopamine release and opposes Parkinson disease-related neurodegeneration *in vivo*. Proc. Natl. Acad. Sci. USA *111*, 9977–9982. https://doi.org/10.1073/pnas.1402134111.

56. Masato, A., Plotegher, N., Boassa, D., and Bubacco, L. (2019). Impaired dopamine metabolism in Parkinson's disease pathogenesis. Mol. Neurodegener. *14*, 35. https://doi.org/10.1186/s13024-019-0332-6.

57. Zhang, J., Perry, G., Smith, M.A., Robertson, D., Olson, S.J., Graham, D.G., and Montine, T.J. (1999). Parkinson's disease is associated with oxidative damage to cytoplasmic DNA and RNA in substantia nigra neurons. Am. J. Pathol. *154*, 1423–1429. https://doi.org/10.1016/S0002-9440(10)65396-5.

58. Spencer, J.P., Jenner, A., Aruoma, O.I., Evans, P.J., Kaur, H., Dexter, D.T., Jenner, P., Lees, A.J., Marsden, D.C., and Halliwell, B. (1994). Intense oxidative DNA damage promoted by L-dopa and its metabolites. Implications for neurodegenerative disease. FEBS Lett. *353*, 246–250. https://doi.org/10.1016/0014-5793(94)01056-0.

59. Bisaglia, M., Filograna, R., Beltramini, M., and Bubacco, L. (2014). Are dopamine derivatives implicated in the pathogenesis of Parkinson's disease? Ageing Res. Rev. *13*, 107–114. https://doi.org/10.1016/j.arr.2013.12.009.

60. Stansley, B.J., and Yamamoto, B.K. (2013). L-dopa-induced dopamine synthesis and oxidative stress in serotonergic cells. Neuropharmacology *67*, 243–251. https://doi.org/10.1016/j.neuropharm.2012.11.010.

61. Maharaj, H., Sukhdev Maharaj, D., Scheepers, M., Mokokong, R., and Daya, S. (2005). l-DOPA administration enhances 6-hydroxydopamine generation. Brain Res. *1063*, 180–186. https://doi.org/10.1016/j.brainres.2005.09.041.

62. Chen, S.H., Kuo, C.W., Lin, T.K., Tsai, M.H., and Liou, C.W. (2020). Dopamine Therapy and the Regulation of Oxidative Stress and Mitochondrial DNA Copy Number in Patients with Parkinson's Disease. Antioxidants *9*, 1159. https://doi.org/10.3390/antiox9111159.

63. Lipski, J., Nistico, R., Berretta, N., Guatteo, E., Bernardi, G., and Mercuri, N.B. (2011). L-DOPA: a scapegoat for accelerated neurodegeneration in Parkinson's disease? Prog. Neurobiol. *94*, 389–407. https://doi.org/10.1016/j.pneurobio.2011.06.005.

64. Carmichael, K., Sullivan, B., Lopez, E., Sun, L., and Cai, H. (2021). Diverse midbrain dopaminergic neuron subtypes and implications for complex clinical symptoms of Parkinson's disease. Ageing Neurodegener. Dis. *1*. https://doi.org/10.20517/and.2021.07.

65. Matsuda, W., Furuta, T., Nakamura, K.C., Hioki, H., Fujiyama, F., Arai, R., and Kaneko, T. (2009). Single nigrostriatal dopaminergic neurons form widely spread and highly dense axonal arborizations in the neostriatum. J. Neurosci. *29*, 444–453. https://doi.org/10.1523/JNEUROSCI.4029-08.2009.

66. Mattson, M.P., and Magnus, T. (2006). Ageing and neuronal vulnerability. Nat. Rev. Neurosci. *7*, 278–294. https://doi.org/10.1038/nrn1886.

67. Ma, S.Y., Rinne, J.O., Collan, Y., Röyttä, M., and Rinne, U.K. (1996). A quantitative morphometrical study of neuron degeneration in the substantia nigra in Parkinson's disease. J. Neurol. Sci. *140*, 40–45. https://doi.org/10.1016/0022-510x(96)00069-x.

68. Bockstael, O., Chtarto, A., Wakkinen, J., Yang, X., Melas, C., Levivier, M., Brotchi, J., and Tenenbaum, L. (2008). Differential transgene expression profiles in rat brain, using rAAV2/1 vectors with tetracycline-inducible and cytomegalovirus promoters. Hum. Gene Ther. *19*, 1293–1305.

69. Turconi, G., Kopra, J., Võikar, V., Kulesskaya, N., Vilenius, C., Piepponen, T.P., and Andressoo, J.O. (2020). Chronic 2-Fold Elevation of Endogenous GDNF Levels Is Safe and Enhances Motor and Dopaminergic Function in Aged Mice. Mol. Ther. Methods Clin. Dev. *17*, 831–842. https://doi.org/10.1016/j.omtm.2020.04.003.

70. Nutt, J.G., Burchiel, K.J., Comella, C.L., Jankovic, J., Lang, A.E., Laws, E.R., Jr., Lozano, A.M., Penn, R.D., Simpson, R.K., Jr., Stacy, M., et al. (2003). Randomized, double-blind trial of glial cell line-derived neurotrophic factor (GDNF) in PD. Neurology *60*, 69–73.

71. Quintino, L., Namislo, A., Davidsson, M., Breger, L.S., Kavanagh, P., Avallone, M., Elgstrand-Wettergren, E., Isaksson, C., and Lundberg, C. (2018). Destabilizing Domains Enable Long-Term and Inert Regulation of GDNF Expression in the Brain. Mol. Ther. Methods Clin. Dev. *11*, 29–39. https://doi.org/10.1016/j.omtm.2018.08.008.

72. Manfredsson, F.P., Bloom, D.C., and Mandel, R.J. (2012). Regulated protein expression for *in vivo* gene therapy for neurological disorders: Progress, strategies, and issues. Neurobiol. Dis. *48*, 212–221. https://doi.org/10.1016/j.nbd.2012.03.001.

73. Chtarto, A., Bockstael, O., Tshibangu, T., Dewitte, O., Levivier, M., and Tenenbaum, L. (2013). A next step in adeno-associated virus-mediated gene therapy for neurological diseases: regulation and targeting. Br. J. Clin. Pharmacol. *76*, 217–232. https://doi.org/10.1111/bcp.12065.

74. Cheng, S., Tereshchenko, J., Zimmer, V., Vachey, G., Pythoud, C., Rey, M., Liefhebber, J., Raina, A., Streit, F., Mazur, A., et al. (2018). Therapeutic efficacy of regulable GDNF expression for Huntington's and Parkinson's disease by a high-induction, background-free "GeneSwitch" vector. Exp. Neurol. *309*, 79–90. https://doi.org/10.1016/j.expneurol.2018.07.017.

75. Manfredsson, F.P., Burger, C., Rising, A.C., Zuobi-Hasona, K., Sullivan, L.F., Lewin, A.S., Huang, J., Piercefield, E., Muzyczka, N., and Mandel, R.J. (2009). Tight Long-term dynamic doxycycline responsive nigrostriatal GDNF using a single rAAV vector. Mol. Ther. *17*, 1857–1867. https://doi.org/10.1038/mt.2009.196.

76. Chtarto, A., Yang, X., Bockstael, O., Melas, C., Blum, D., Lehtonen, E., Abeloos, L., Jaspar, J.M., Levivier, M., Brotchi, J., et al. (2007). Controlled delivery of glial cell line-derived neurotrophic factor by a single tetracycline-inducible AAV vector. Exp. Neurol. *204*, 387–399. https://doi.org/10.1016/j.expneurol.2006.11.014.

77. Quintino, L., Manfré, G., Wettergren, E.E., Namislo, A., Isaksson, C., and Lundberg, C. (2013). Functional neuroprotection and efficient regulation of GDNF using destabilizing domains in a rodent model of Parkinson's disease. Mol. Ther. *21*, 2169–2180. https://doi.org/10.1038/mt.2013.169.

78. Cheng, S., van Gaalen, M.M., Bähr, M., Garea-Rodriguez, E., and Kügler, S. (2021). Optimized pharmacological control over the AAV-Gene-Switch vector for regulable gene therapy. Mol. Ther. Methods Clin. Dev. *23*, 1–10. https://doi.org/10.1016/j.omtm.2021.07.007.

79. Walker, C., Preshaw, P.M., Novak, J., Hefti, A.F., Bradshaw, M., and Powala, C. (2005). Long-term treatment with sub-antimicrobial dose doxycycline has no antibacterial effect on intestinal flora. J. Clin. Periodontol. *32*, 1163–1169. https://doi.org/10.1111/j.1600-051X.2005.00840.x.

80. Walker, C., Thomas, J., Nangó, S., Lennon, J., Wetzel, J., and Powala, C. (2000). Long-term treatment with subantimicrobial dose doxycycline exerts no antibacterial effect on the subgingival microflora associated with adult periodontitis. J. Periodontol. *71*, 1465–1471. https://doi.org/10.1902/jop.2000.71.9.1465.

81. Walker, C.B., Godowski, K.C., Borden, L., Lennon, J., Nangó, S., Stone, C., and Garrett, S. (2000). The effects of sustained release doxycycline on the anaerobic flora and antibiotic-resistant patterns in subgingival plaque and saliva. J. Periodontol. *71*, 768–774. https://doi.org/10.1902/jop.2000.71.5.768.

82. Favre, D., Blouin, V., Provost, N., Spisek, R., Porrot, F., Bohl, D., Marmé, F., Chérel, Y., Salvetti, A., Hurtrel, B., et al. (2002). Lack of an immune response against the tetracycline-dependent transactivator correlates with long-term doxycycline-regulated transgene expression in nonhuman primates after intramuscular injection of recombinant adeno-associated virus. J. Virol. *76*, 11605–11611.

83. Xiong, W., Candolfi, M., Kroeger, K.M., Puntel, M., Mondkar, S., Larocque, D., Liu, C., Curtin, J.F., Palmer, D., Ng, P., et al. (2008). Immunization against the transgene but not the TetON switch reduces expression from gutless adenoviral vectors in the brain. Mol. Ther. *16*, 343–351. https://doi.org/10.1038/sj.mt.6300375.

84. Stieger, K., Le Meur, G., Lasne, F., Weber, M., Deschamps, J.Y., Nivard, D., Mendes-Madeira, A., Provost, N., Martin, L., Moullier, P., and Rolling, F. (2006). Long-term doxycycline-regulated transgene expression in the retina of nonhuman primates following subretinal injection of recombinant AAV vectors. Mol. Ther. *13*, 967–975. https://doi.org/10.1016/j.ymthe.2005.12.001.

85. Tang, C.X., Chen, J., Shao, K.Q., Liu, Y.H., Zhou, X.Y., Ma, C.C., Liu, M.T., Shi, M.Y., Kambey, P.A., Wang, W., et al. (2023). Blunt dopamine transmission due to decreased GDNF in the PFC evokes cognitive impairment in Parkinson's disease. Neural Regen. Res. *18*, 1107–1117. https://doi.org/10.4103/1673-5374.355816.

86. Zhou, X., Vink, M., Klaver, B., Berkhout, B., and Das, A.T. (2006). Optimization of the Tet-On system for regulated gene expression through viral evolution. Gene Ther. *13*, 1382–1390. https://doi.org/10.1038/sj.gt.3302780.

87. Driessens, G., Nuttin, L., Gras, A., Maetens, J., Mievis, S., Schoore, M., Velu, T., Tenenbaum, L., Préat, V., and Bruyns, C. (2011). Development of a successful anti-tumor therapeutic model combining *in vivo* dendritic cell vaccination with tumor irradiation and intratumoral GM-CSF delivery. Cancer Immunol. Immunother. *60*, 273–281. https://doi.org/10.1007/s00262-010-0941-y.

88. Bockstael, O., Melas, C., Pythoud, C., Levivier, M., McCarty, D., Samulski, R.J., De Witte, O., and Tenenbaum, L. (2012). Rapid transgene expression in multiple precursor cell types of adult rat subventricular zone mediated by adeno-associated type 1 vectors. Hum. Gene Ther. *23*, 742–753. https://doi.org/10.1089/hum.2011.216.

89. Aurnhammer, C., Haase, M., Muether, N., Hausl, M., Rauschhuber, C., Huber, I., Nitschko, H., Busch, U., Sing, A., Ehrhardt, A., and Baiker, A. (2012). Universal real-time PCR for the detection and quantification of adeno-associated virus serotype 2-derived inverted terminal repeat sequences. Hum. Gene Ther. Methods *23*, 18–28. https://doi.org/10.1089/hgtb.2011.034.

90. Penaud-Budloo, M., Lecomte, E., Guy-Duché, A., Saleun, S., Roulet, A., Lopez-Roques, C., Tournaire, B., Cogné, B., Léger, A., Blouin, V., et al. (2017). Accurate Identification and Quantification of DNA Species by Next-Generation Sequencing in Adeno-Associated Viral Vectors Produced in Insect Cells. Hum. Gene Ther. Methods *28*, 148–162. https://doi.org/10.1089/hgtb.2016.185.

91. Paxinos, G., and Watson, C. (1998). The Rat Brain in Stereotaxic Coordinates (Academic Press).

92. Peter, D., Liu, Y., Sternini, C., de Giorgio, R., Brecha, N., and Edwards, R.H. (1995). Differential expression of two vesicular monoamine transporters. J. Neurosci. *15*, 6179–6188.

93. Cruz-Muros, I., Afonso-Oramas, D., Abreu, P., Rodríguez, M., González, M.C., and González-Hernández, T. (2008). Deglycosylation and subcellular redistribution of VMAT2 in the mesostriatal system during normal aging. Neurobiol. Aging *29*, 1702–1711. https://doi.org/10.1016/j.neurobiolaging.2007.04.003.

94. Laganiere, J., Kells, A.P., Lai, J.T., Guschin, D., Paschon, D.E., Meng, X., Fong, L.K., Yu, Q., Rebar, E.J., Gregory, P.D., et al. (2010). An engineered zinc finger protein activator of the endogenous glial cell line-derived neurotrophic factor gene provides functional neuroprotection in a rat model of Parkinson's disease. J. Neurosci. *30*, 16469–16474. https://doi.org/10.1523/JNEUROSCI.2440-10.2010.